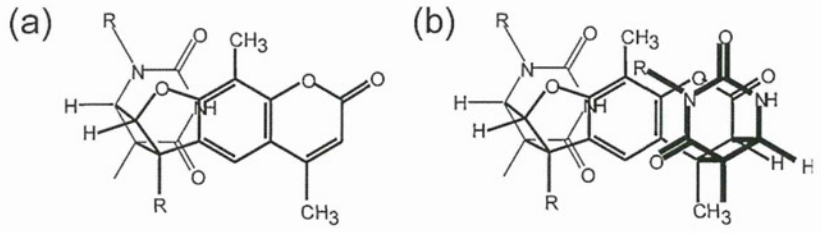

Fig. 21. (a) Photo-crosslinking of pso-ODN with single-stranded DNA and (b) with double-stranded DNA.

steps to form covalently fixed stable triplexes under physiological conditions [147].

The mononuclear ruthenium(II) complexes that contain at least two π-deficient polyazaaromatic ligands such as TAP (1,4,5,8-tetraazaphenenthrene) or HAT(1,4,5,8,9,12-hexaazatriphenylene) are known to behave as oxidizing agent under illumination, and can therefore extract one electron from a guanine (G) base of DNA. The pair of radicals formed after the electron transfer give rise to a covalent adduct involving the Gbase [148,149]. Kirsch-De Mesmaeker et al. introduced the Ru(II) complex ($[Ru(tap)_3]^{2+}$) to an ODN to form the conjugate. UV irradiation of the duplex with the target provided the adduct with G in the vicinity of the attached complex. As a result, the two strands were crosslinked, which inhibited the activities of both an exonuclease [150] and polymerase [151] with high efficiency. They referred to the DNA conjugate as a "seppuku molecule", because it inactivates itself by forming a cyclic form when it cannot find the target [152] (Fig. 22).

o-Quinone methide (*o*-QM) has played important roles in organic synthesis as well as in chemical and biological processes. *o*-QM has significance because of its nucleobase alkylation [153]. Zhou et al. reported a potent, water-soluble and photoinducible DNA crosslinker based on a unique reaction mechanism involving an *o*-QM intermediate. The reagent they prepared was biphenol biquaternary ammonium. Upon visible light irradiation, two ammonium groups are eliminated from the reagent to give an intermediate with two *o*-QM structures, which couple with nucleophiles on nucleobases to form crosslinked duplex DNA [154] (Fig. 23).

4.3. Chemical ligations

DNA ligation usually refers to the enzymatic process in which the termini of the two DNA fragments with phosphate and hydroxyl groups are connected to each other via the formation of a phosphodiester bond on the complementary template DNA. Ligase is the responsible enzyme of this reaction and an essential enzyme in DNA repair, replication, and recombination. Ligation is widely used as a probe reaction for DNA analyses because of its rigorous base recognition. On the other hand, a number of non-enzymatic approaches (chemical ligation) have been developed by several research groups. Chemical methods have possible advantages over enzymatic approaches, especially in analytical and engineering applications. Benefits include reduced cost, greater robustness under various conditions, and higher tolerance to the structures other than DNA duplexes, including duplex terminals, triplexes, quadruplexes, RNA, and nucleic acid analogues. In this section, we focus on autoligation and photochemical ligation. These ligations can be carried out in cells or tissues because they do not require any additives. The reaction of photochemical ligations can be easily controlled by varying the irradiation time, light strength, and wavelength.

4.3.1. Autoligation

Letsinger and co-workers reported the first autoligation of short DNA fragments bearing electrophilic bromoacetoamido and nucleophilic phosphorothioate groups [155]. The reaction yields were reduced 15-fold by the presence of a single nucleotide mismatch. The reaction proceeded on a triple-helix structure [156]. Kool et al. introduced a fluorescence signal synchronizing with the reaction using three autoligating energy transfer (ALET) probes. Each of the ALET probes carries different fluorescent dyes that function as FRET donors and acceptors. The two probes that were complementary to the target were observed to connect by spontaneous phosphorothioate-iodide ligation. Multiple detection can be carried out with a color change based on specific FRET on

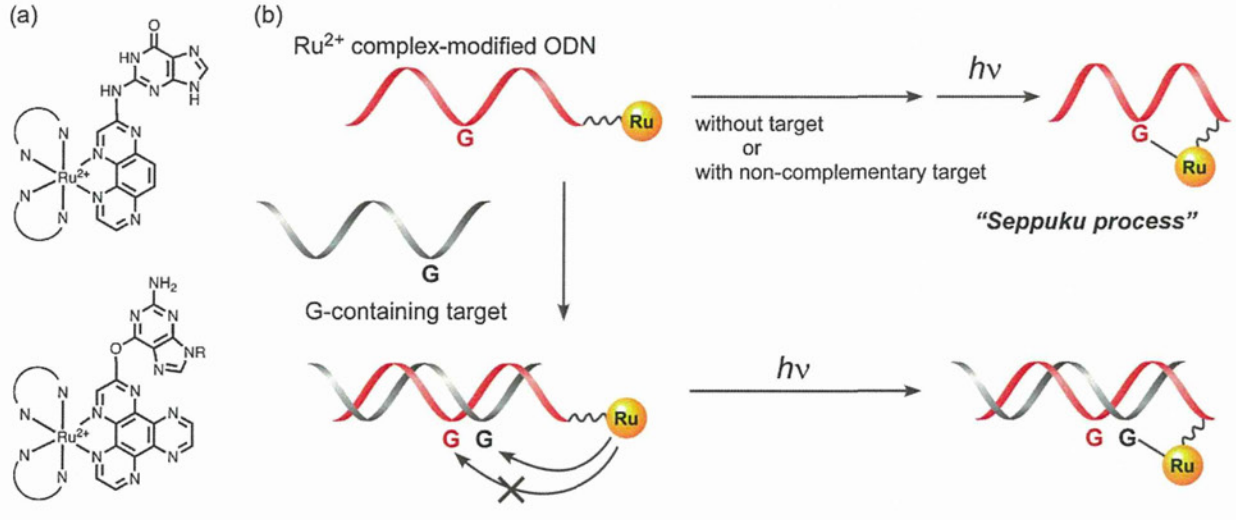

Fig. 22. (a) Structures of the photoadducts of the Ru^{2+} complexes consisting of a TAP ligand with a G base and a HAT ligand with a guanosine monophosphate (R = phosphoribose). (b) Schematic representation of the photochemical behavior of a Ru^{2+} complex-modified ODN in the absence and in the presence of G-containing target strands.

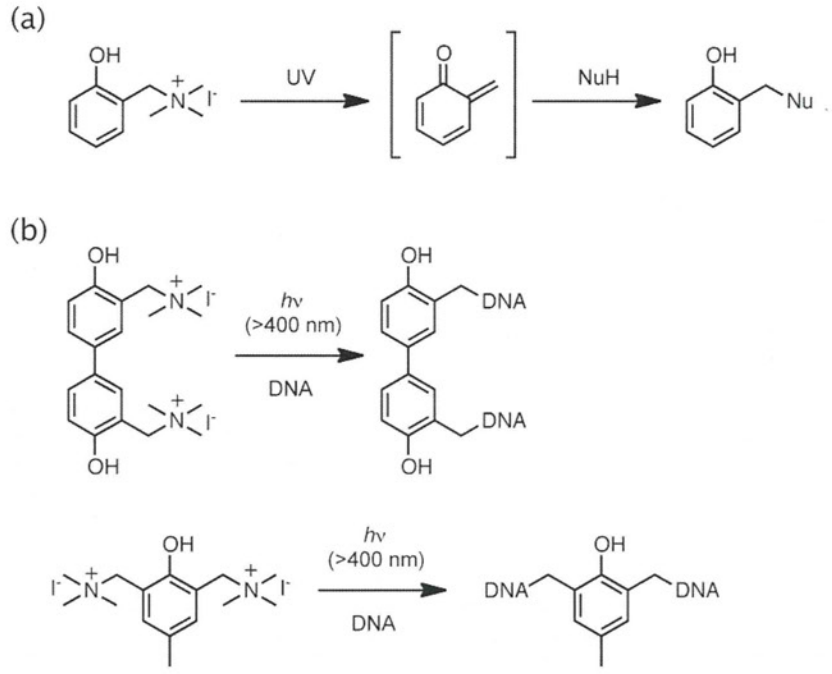

Fig. 23. (a) *o*-QM formation by photoactivation. (b) Photo-triggered DNA crosslinking by *o*-QM derivatives.

ligated products [157]. They extended the system to quenched autoligation (QUAL). The leaving group in the ALET probe, iodide, was substituted with the FRET quencher, dabsyl (dimethylamino-azobenzenesulfonyl). The fluorescence signal is restored with the ligating reaction. Multiple assays are also possible in this system using a combination of several QUAL probes [158,159] (Fig. 24).

4.3.2. [2π–2π] photochemical ligations

Successive thymines in the same strand form a dimer via cyclobutane formation ([2π–2π] cycloaddition) under UV irradiation. Skin cancer results if the dimers remain to be repaired and accumulate (Fig. 25). This chemistry was used for the first photochemical ligations by Lewis and Hanawalt [160]. Liu and Taylor substituted thymines at ligation sites with 4-thiothymines to shift

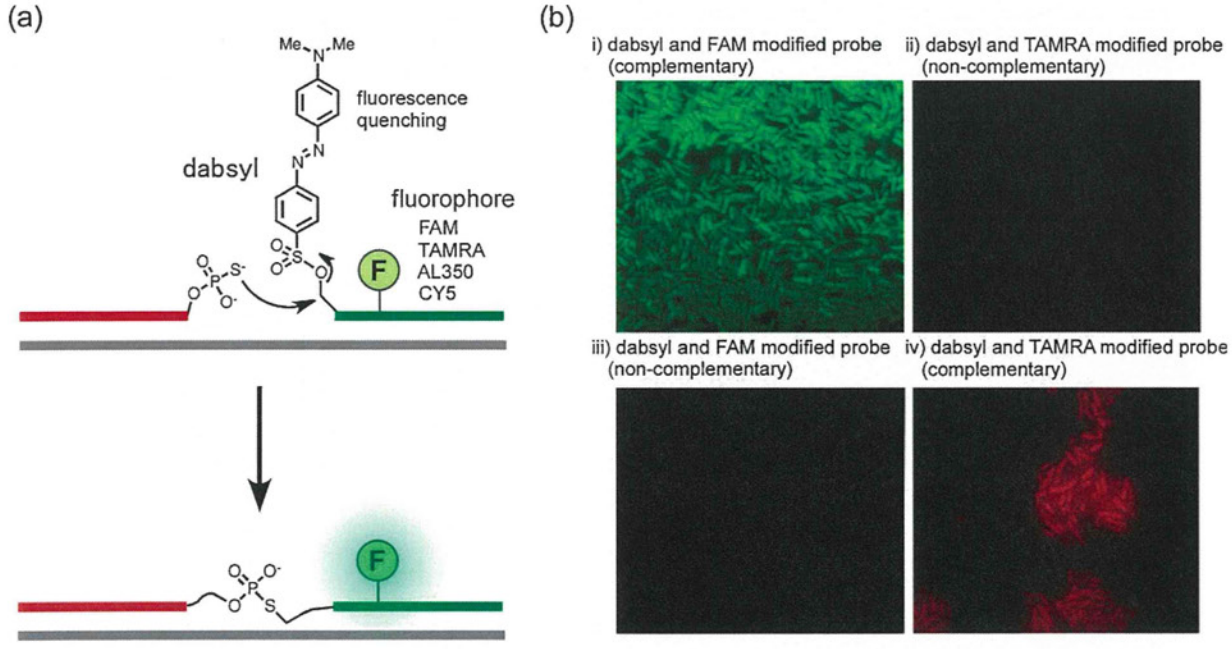

Fig. 24. (a) Schematic showing the signal generation in the QUAL system. (b) Single nucleotide discrimination by two-color autoligation. Fixed *Escherichia coli* cells (MG1655 strain) were incubated for 18 h at 37 °C with (i) dabsyl and the FAM-modified ODN probe (complementary to the target), (ii) dabsyl and the FAM-modified ODN probe (non-complementary to the target), (iii) dabsyl and the TAMRA-modified ODN probe (complementary to the target), and (iv) dabsyl and the TAMRA-modified ODN probe (non-complementary to the target) in the presence of both a phosphorothioate ODN probe and a helper ODN (assists in the hybridization of the probes in regions of strong secondary structure). FAM and TAMRA were excited at 460–500 nm (left) and 530–560 nm (right) wavelengths, respectively.
Reprinted from [158] with permission from the American Chemical Society.

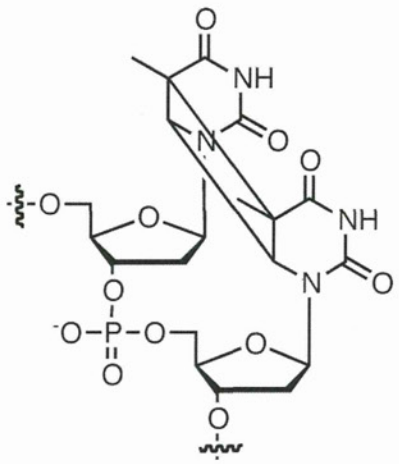

Fig. 25. Structure of a thymine dimer.

the wavelength of irradiation to longer wavelengths. Sequence specific ligation was observed by 366 nm irradiation without significant damage of canonical nucleobases [161]. Albagli et al. reported the chemical amplification of ligation products by self-replication with repeated thermal cycles. They prepared a DNA conjugate carrying coumarin in the DNA backbone. The ligation proceeded by cycloaddition between the coumarin and a vicinal thymine on opposite strand located in an arm of a three-way-junction [162].

Fujimoto et al. succeeded in a series of photochemical ligations by cyclobutane dimer formation of modified nucleobases with vinyl groups. They reported template-directed reversible photochemical ligation via 5-vinylpyrimidine. Upon irradiation of 366 nm, the vinylpyrimidine attached to the 5′-end of the ODN joined with pyrimidine at the 3′-end of another ODN hybridized to an adjacent site on the template. The reaction was reversible by 302 nm irradiation [163] (Fig. 26). Cognate reactions have been carried out to form various structures such as blanched [164], circular [165], catenated [166], and R-shaped DNA [167]. SNP genotyping with high sensitivity and selectivity was reported using allele-specific hybridization with a DNA array on a chip. The signal contrast for the targets with a point mutation was >10^3-fold higher [168]. RNA analysis was also performed successfully using the same format [169]. The reaction was used to discriminate 5-methylcytosine from cytosine. 5-Methylcytosine is an important target in epigenetics. High selectivity of the reaction yield was based on the difference in stacking stability induced by the hydrophobic interactions of the methyl group [170]. The techniques can also be extended as a tool for genetic engineering. Site-specific transition of cytosine to uracil was performed by heat-induced deamination of the cytosine residue of a cyclobutane dimer followed by splitting [171]. A one-pot autonomous DNA computing machine was constructed using the photochemically induced gate transition, which is based on site-specific photocleavage, hybridization, and ligation [172,173].

4.3.3. [4π–4π] photochemical ligations

Anthracene readily forms photo-adducts, anthracene dimers, and this photodimerization reaction ([4π–4π] cycloaddition) has been characterized in detail. The reactivities of many anthracene derivatives under various conditions have been studied extensively. Although the yields of anthracene dimer formation in diluted solutions are generally low, the reactions proceed efficiently under particular conditions, such as in the cavity of cyclodextrin, because of the concentration effect in a microenvironment [174–176]. DNA should function as a good scaffold to provide such a microenvironment, because a DNA scaffold allows us to design the system so that the reaction partners (two anthracenes) are located in close proximity and appropriate spatial alignment.

Ihara et al. attached an anthracene group as a handle to one end of each of a number of ODNs to form anthracene–ODN conjugates [177–181]. Upon irradiation at 366 nm, the anthracene dimer formed in the presence of a complementary template (analyte). The reaction was almost complete in a few seconds and sequence specificity was high. This reaction may be suitable as a probe reaction for convenient SNP assays [177–179] (Fig. 27). Undesired cross-linking reactions with nucleobases (pyrimidines) were not observed, because the photoreaction involving anthracene isorthogonal to the typical [2π + 2π] reaction that nucleobases take part in. The reaction proceeded not only on a tandem duplex but also other structures such as the end of duplexes and triplexes [180]. Circularization was performed using the conjugates carrying two anthracenes, one on each end, in the presence of the template. The reaction was reversible by 312 nm irradiation [181] (Fig. 28). The system should also be useful as a fundamental reaction for the construction of molecular nanostructures.

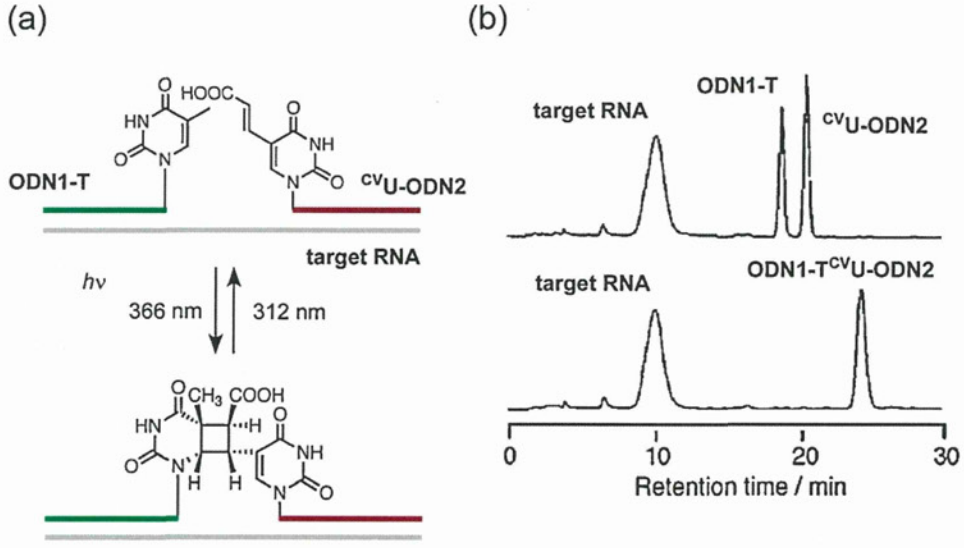

Fig. 26. (a) Schematic representation of RNA-directed photoreversible ligation. (b) HPLC analysis of the solution containing ^{CV}U-ODN2, ODN-T, and template RNA before (upper) or after (under) irradiation at 366 nm for 30 min (reprinted from [169] with permission from Wiley-VCH Verlag GmbH & Co. KGaA).

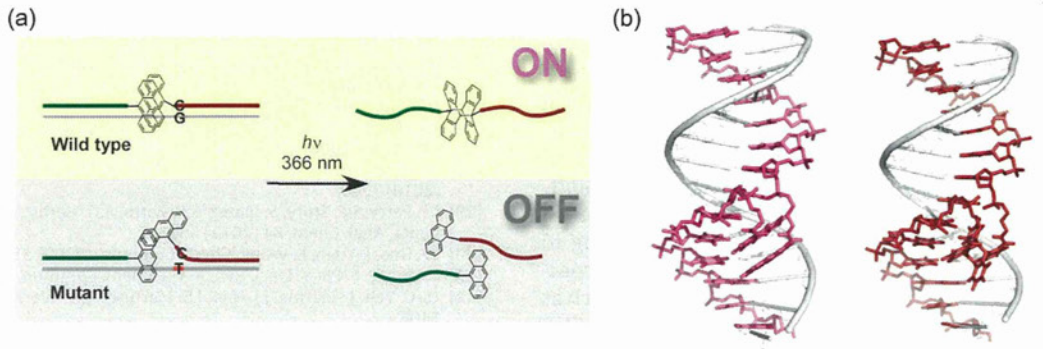

Fig. 27. (a) DNA-templated photochemical ligation of anthracene-modified ODN through cyclodimer formation. (b) Possible structures of the duplexes formed between anthracene-modified ODNs and target ODN before (left) and after (right) photo-irradiation.

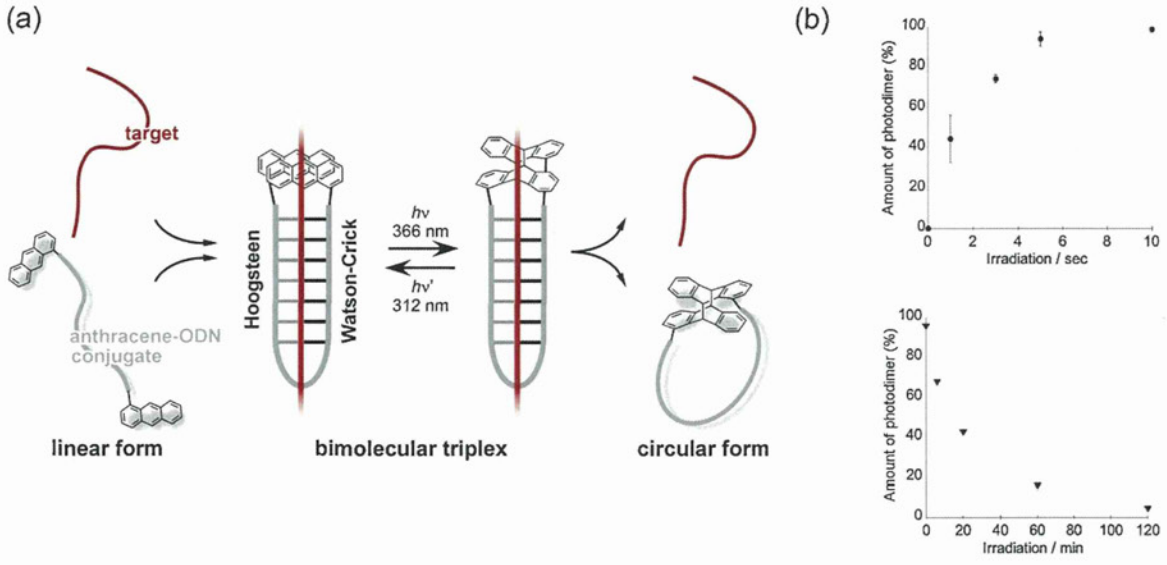

Fig. 28. (a) Reversible circularization of an anthracene-modified DNA conjugate through bimolecular triplex formation. (b) The time course of the photoreactions. Upper: The photoligation (circularization) of bimolecular triplexes in the presence of the target. Reaction mixtures contained 3.3 μM of heptamer targets and 2.2 μM of anthracene-modified ODN in 100 mM sodium acetate buffer (pH 5.0, 10 mM NaCl, 10 mM $MgCl_2$). Lower: Time course for the photodissociation of an anthracene photodimer upon irradiation at 312 nm.

5. Conclusions

This review summarized photochemically relevant DNA assemblies mainly reported over the last few years. DNA is a well-behaved molecule. There are several advantages for using DNA as a scaffold or template in the design of the molecular assemblies with specific functions. These include:

(1) *The structure of DNA is characterized by its regularity, i.e., pitch of the helix, twist and rise of stacking nucleobases, and the distance between anionic charges.* Various organic molecules, metal complexes, and metal ions assemble along the DNA duplex template to form well-defined 1D nanostructures with unique properties.
(2) *DNA is chemically stable. The techniques of DNA preparation are well established.* DNA can be prepared in nearly any length and sequence by chemical and enzymatic syntheses. Auxiliary functional groups can be built into the backbone as amidite reagents. In addition, we can choose appropriate methods from an abundant range of specific chemistries that carried outpost-modification.
(3) *The structures of DNA are programmable.* The conditions required (pH, ionic strength, temperature) for the formation of each of the structural units of DNA, e.g., hairpins, duplexes, triplexes, quadruplexes, and the i-motif, are well established. Desired DNA structures, in which the functional groups are located at defined positions, can be spontaneously organized under particular conditions. Critical parameters for obtaining particular DNA structures are only the sequences of the constituents and the conditions of the solution. Allosteric binary motion of a part of the hierarchically arranged DNA structures can be realized by careful design of the systems.

The studies for DNA-templated functional molecular assemblies have rapidly expanded over the last decade because of the advantages of DNA as building blocks or materials as mentioned above, and the bioorthogonal reactions that are now available. This research area is still in its infancy. The development of this field will contribute to bioanalyses, nanomachines, and nanomaterials.

Several issues should be considered in the study of DNA-templated functional molecular assemblies. For some purposes, the systems are very useful for in vitro assay. While, the applications in vivo are rather beneficial for the research of life sciences. The functional assemblies would be strong research tools for spatiotemporal imaging. Photochemistry is intrinsically selective. It does not require any additives. Meanwhile, several bioorthogonal

chemical reactions that proceed in aqueous media under mild conditions have recently become available. Combined use of these chemistries should facilitate in vivo applications of this method. Signal amplification is also important. It would be one of the critical requirement for in vivo applications. The design of effective chemical or autonomous signal amplification that does not depend on specific enzymes may represent a promising solution. The quantities (=cost) of the assemblies that we can prepare are of interest when they are regarded as materials. It is rather challenging to obtain bulk amounts of the assemblies. The sensitivity of the combined measuring method is important. The use of bulk DNA such as from calf thymus or salmon testis, or DNA analogues such as PNA may circumvent this potential bottleneck.

All of the studies covered in this review are highly interdisciplinary. They are the "assemblies" of several different research areas such as photochemistry, biochemistry, organic synthesis, inorganic chemistry, materials science, and analytical science. Advances in particular research areas are likely to affect other disciplines and inspire further development and improvements. Consequently, it is likely that such a cooperative effect will make a significant difference ("amplification") in the performance of integrated studies, such as those covered in this review.

Acknowledgments

We acknowledge support from the Ministry of Education, Culture, Sports, Science and Technology (MEXT), Japan Science and Technology Agency (JST), and the Ministry of Health, Labour and Welfare (MHLW).

References

[1] J.D. Watson, F.H. Crick, Nature 171 (1953) 737.
[2] International Human Genome Sequencing Consortium, Nature 409 (2001) 860.
[3] J.C. Venter, et al., Science 291 (2001) 1304.
[4] For example E.S. Lander, Nature 470 (2011) 187.
[5] H. Gu, J. Chao, S.-J. Xiao, N.C. Seeman, Nature 465 (2010) 202.
[6] J. Bath, A.J. Turberfield, Nat. Biotechnol. 2 (2007) 275.
[7] B. Saccà, C.M. Niemeyer, Angew. Chem. Int. Ed. 51 (2012) 58.
[8] A. Rajendran, M. Endo, H. Sugiyama, Angew. Chem. Int. Ed. 51 (2012) 874.
[9] J. Liu, Z. Cao, Y. Lu, Chem. Rev. 109 (2009) 1948.
[10] J.L. Vinkenborg, N. Karnowski, M. Famulok, Nat. Chem. Biol. 7 (2011) 519.
[11] I. Willner, M. Zayats, Angew. Chem. Int. Ed. 46 (2007) 6408.
[12] A.B. Iliuk, L. Hu, W.A. Tao, Anal. Chem. 83 (2011) 4440.
[13] S. Tyagi, F.R. Kramer, Nat. Biotechnol. 14 (1996) 303.
[14] K. Wang, Z. Tang, C.J. Yang, Y. Kim, X. Fang, W. Li, Y. Wu, C.D. Medley, Z. Cao, J. Li, P. Colon, H. Lin, W. Tan, Angew. Chem. Int. Ed. 48 (2009) 856.
[15] D.M. Kolpashchikov, Chem. Rev. 110 (2010) 4709.
[16] S.K. Silverman, Angew. Chem. Int. Ed. 49 (2010) 7180.
[17] S. Park, H. Sugiyama, Angew. Chem. Int. Ed. 49 (2010) 3870.
[18] R.K.V. Lim, Q. Lin, Chem. Commun. 46 (2010) 1589.
[19] R. Garoff, E.A. Litzinger, R.E. Connor, I. Fishman, B.A. Armitage, Langmuir 18 (2002) 6330.
[20] K.C. Hannar, B.A. Armitage, Acc. Chem. Res. 37 (2004) 845.
[21] H.J. Carlsson, M. Erikson, E. Perzon, B. Åkerman, P. Lincoln, G. Westman, Nucleic Acids Res. 31 (2003) 6227.
[22] T. Ihara, T. Ikegami, T. Fujii, Y. Kitamura, S. Sueda, M. Takagi, A. Jyo, J. Inorg. Chem. 100 (2006) 1744.
[23] L.-A. Fendt, I. Bouamaied, S. Thöni, N. Amiot, E. Stulz, J. Am. Chem. Soc. 129 (2007) 15319.
[24] T.N. Nguyen, A. Brewer, E. Stulz, Angew. Chem. Int. Ed. 48 (2009) 1974.
[25] E. Mayer-Enthart, C. Wagner, J. Barbaric, H.-A. Wagenknecht, Tetrahedron 63 (2007) 3434.
[26] M. Nakamura, Y. Murakami, K. Sasa, H. Hayashi, K. Yamana, J. Am. Chem. Soc. 130 (2008) 6904.
[27] Y.N. Teo, J.N. Wilson, E.T. Kool, J. Am. Chem. Soc. 131 (2009) 3923.
[28] S.S. Tan, S.J. Kim, E.T. Kool, J. Am. Chem. Soc. 133 (2011) 2664.
[29] H. Kashida, K. Sekiguchi, X. Liang, H. Asanuma, J. Am. Chem. Soc. 132 (2010) 6223.
[30] F. Garo, R. Häner, Angew. Chem. Int. Ed. 51 (2012) 916.
[31] C. Song, Y.-Q. Chen, S.-J. Xiao, L. Ba, Z.-Z. Gu, Y. Pan, X.-Z. You, Chem. Mater. 17 (2005) 6521.
[32] E. Braun, Y. Eichen, U. Sivan, G. Ben-Yoseph, Nature 391 (1998) 775.
[33] C.T. Wirges, J. Timper, M. Fischler, A.S. Sologubenko, J. Mayer, U. Simon, T. Carell, Angew. Chem. Int. Ed. 48 (2009) 219.
[34] R. Schreiber, S. Kempter, S. Holler, V. Schüller, D. Schiffels, S.S. Simmel, P.C. Nickels, T. Liedl, Small 7 (2011) 1795.
[35] M. Fischler, U. Simon, H. Nir, Y. Eichen, G.A. Burley, J. Gierlich, P.M.E. Gramlich, T. Carell, Small 3 (2007) 1049.
[36] W. Guo, J. Yuan, Q. Dong, E. Wang, J. Am. Chem. Soc 132 (2010) 932.
[37] E.G. Gwinn, P. O'Neill, A.J. Guerrero, D. Bouwmeester, D.K. Fygenson, Adv. Mater. 20 (2008) 279.
[38] J. Sharma, H.-C. Yeh, H. Yoo, J.H. Werner, J.S. Martinez, Chem. Commun. 46 (2010) 3280.
[39] J.T. Petty, S.P. Story, S. Juarez, S.S. Votto, A.G. Herbst, N.N. Degtyareva, B. Sengupta, Anal. Chem. 84 (2012) 356.
[40] W. Guo, J. Yuan, E. Wang, Chem. Commun. (2009) 3395.
[41] Z. Huang, F. Pu, Y. Lin, J. Ren, X. Qu, Chem. Commun. 47 (2011) 3487.
[42] H.-C. Yeh, J. Sharma, J.J. Han, J.S. Martinez, J.H. Werner, Nano Lett. 10 (2010) 3106.
[43] J.H. Yu, S. Choi, R.M. Dickson, Angew. Chem. Int. Ed. 48 (2009) 318.
[44] A. Rotaru, S. Dutta, E. Jentzsch, K. Gothelf, A. Mokhir, Angew. Chem. Int. Ed. 49 (2010) 5665.
[45] J. Chen, J. Liu, Z. Fang, L. Zeng, Chem. Commun. 48 (2012) 1057.
[46] Z. Zhou, Y. Du, S. Dong, Anal. Chem. 83 (2011) 5122.
[47] G.H. Clever, C. Kaul, T. Carell, Angew. Chem. Int. Ed. 46 (2007) 6226.
[48] S. Ghosh, E. Defrancq, Chem. Eur. J. 16 (2010) 12780.
[49] K. Tanaka, A. Tengeiji, T. Kato, N. Toyama, M. Shionoya, Science 299 (2003) 1212.
[50] K. Tanaka, G.H. Clever, Y. Takezawa, Y. Yamada, C. Kaul, M. Shionoya, T. Carell, Nat. Nanotechnol. 1 (2006) 190.
[51] Y. Miyake, H. Togashi, M. Tashiro, H. Yamaguchi, S. Oda, M. Kudo, Y. Tanaka, Y. Kondo, R. Sawa, T. Fujimoto, T. Machinami, A. Ono, J. Am. Chem. Soc. 128 (2006) 2172.
[52] T. Ihara, T. Ishii, N. Araki, A.W. Wilson, A. Jyo, J. Am. Chem. Soc. 131 (2009) 3826.
[53] J. Liu, Y. Lu, Angew. Chem. Int. Ed. 46 (2007) 7587.
[54] S. Cai, K. Lao, C. Lau, J. Lu, Anal. Chem. 83 (2011) 9702.
[55] Y. Wang, J. Li, H. Wang, J. Jin, J. Liu, K. Wang, W. Tan, R. Yang, Anal. Chem. 82 (2010) 6607.
[56] C.X. Tang, N.N. Bu, X.W. He, X.B. Yin, Chem. Commun. 47 (2011) 12304.
[57] J.G. Schmidt, P.E. Nielsen, L.E. Orgel, J. Am. Chem. Soc. 119 (1997) 1494.
[58] X. Li, Z.-Y.J. Zhan, R. Knipe, D.G. Lynn, J. Am. Chem. Soc. 124 (2002) 746.
[59] R.E. Kleiner, Y. Brudno, M.E. Birnbaum, D.R. Liu, J. Am. Chem. Soc. 130 (2008) 4646.
[60] R. Nagarajan, W. Liu, J. Kumar, S.K. Tripathy, F.F. Bruno, L.A. Samuelson, Macromolecules 34 (2001) 3921.
[61] P. Nickels, W.U. Dittmer, S. Beyer, J.P. Kotthaus, F.C. Simmel, Nanotechnol. 15 (2004) 1524.
[62] J. Hannant, J.H. Hedley, J. Pate, A. Walli, S.A. Farha Al-Said, M.A. Galindo, B.A. Connolly, B.R. Horrocks, A. Houltona, A.R. Pike, Chem. Commun. 46 (2010) 5870.
[63] Y. Ma, J. Zhang, G. Zhang, H. He, J. Am. Chem. Soc. 126 (2004) 7097.
[64] B. Datta, G.B. Schuster, A. McCook, S.C. Harvey, K. Zakrzewska, J. Am. Chem. Soc. 128 (2006) 14428.
[65] B. Datta, G.B. Schuster, J. Am. Chem. Soc. 130 (2008) 2965.
[66] S. Srinivasan, G.B. Schuster, Org. Lett. 10 (2008) 3657.
[67] W. Chen, G. Güler, E. Kuruvilla, G.B. Schuster, H.-C. Chiu, E. Riedo, Macromolecules 43 (2010) 4032.
[68] W. Chen, G.B. Schuster, J. Am. Chem. Soc. 134 (2012) 840.
[69] S. Sueda, T. Ihara, M. Takagi, Chem. Lett. 26 (1997) 1085.
[70] S. Sueda, T. Ihara, B. Juskowiak, M. Takagi, Anal. Chim. Acta 365 (1998) 27.
[71] T. Ihara, Y. Takeda, A. Jyo, J. Am. Chem. Soc. 123 (2001) 1772.
[72] M. Göritz, R. Krämer, J. Am. Chem. Soc. 127 (2005) 18016.
[73] N. Graf, M. Göritz, R. Krämer, Angew. Chem. Int. Ed. 45 (2006) 4013.
[74] N. Graf, R. Krämer, Chem. Commun. (2006) 4375.
[75] T. Ehrenschwender, A. Barth, H. Puchta, H.-A. Wagenknecht, Org. Biomol. Chem. 10 (2012) 46.
[76] L. Kalachova, R. Pohl, M. Hocek, Org. Biomol. Chem. 10 (2012) 49.
[77] H. Yang, A.Z. Rys, C.K. McLaughlin, H.F. Sleiman, Angew. Chem. Int. Ed. 48 (2009) 9919.
[78] H. Yang, F. Altvater, A.D. de Bruijn, C.K. McLaughlin, P.K. Lo, H.F. Sleiman, Angew. Chem. Int. Ed. 50 (2011) 4620.
[79] T. Ihara, M. Mukae, Anal. Sci. 23 (2007) 625.
[80] Y. Kitamura, T. Ihara, Y. Tsujimura, M. Tazaki, A. Jyo, Chem. Lett. 34 (2005) 1606.
[81] Y. Kitamura, T. Ihara, Y. Tsujimura, Y. Osawa, M. Tazaki, Anal. Biochem. 359 (2006) 259.
[82] Y. Kitamura, T. Ihara, Y. Tsujimura, Y. Osawa, D. Sasahara, M. Yamamoto, K. Okada, M. Tazaki, A. Jyo, J. Inorg. Biochem. 102 (2008) 1921.
[83] T. Ihara, Y. Kitamura, Y. Tsujimura, A. Jyo, Anal. Sci. 27 (2011) 585.
[84] F.H. Zelder, J. Brunner, R. Krämer, Chem. Commun. (2004) 902.
[85] J. Brunner, A. Mokhir, R. Krämer, J. Am. Chem. Soc. 125 (2003) 12410.
[86] I. Boll, R. Krämer, J. Brunner, A. Mokhir, J. Am. Chem. Soc. 127 (2005) 7849.
[87] J. Brunner, R. Krämer, J. Am. Chem. Soc. 126 (2004) 13626.
[88] G.T. Hermanson, Bioconjugate Techniques, Academic Press, San Diego, CA, 1996, pp. 137–166.
[89] H. Staudinger, J. Meyer, Helv. Chim. Acta 2 (1919) 635.
[90] Y.G. Gololobov, L.F. Kasukhin, Tetrahedron 48 (1992) 1353.
[91] E. Saxon, C.R. Bertozzi, Science 287 (2000) 2007.
[92] M. Köhn, R. Breinbauer, Angew. Chem. Int. Ed. 43 (2004) 3106.

[93] J. Cai, X. Li, X. Yue, J.-S. Taylor, J. Am. Chem. Soc. 126 (2004) 16324.
[94] Z.L. Pianowski, N. Winssinger, Chem. Commun. (2007) 3820.
[95] H. Abe, J. Wang, K. Furukawa, K. Oki, M. Uda, S. Tsuneda, Y. Ito, Bioconjug. Chem. 19 (2008) 1219.
[96] Z.L. Pianowski, K. Gorska, L. Oswald, C.A. Merten, N. Winssinger, J. Am. Chem. Soc. 131 (2009) 6492.
[97] K. Furukawa, H. Abe, K. Hibino, Y. Sako, S. Tsuneda, Y. Ito, Bioconjug. Chem. 20 (2009) 1026.
[98] K. Furukawa, H. Abe, Y. Tamura, R. Yoshimoto, M. Yoshida, S. Tsuneda, Y. Ito, Angew. Chem. Int. Ed. 50 (2011) 12020.
[99] C. Crey-Desbiolles, D.R. Ahn, C.J. Leumann, Nucleic Acids Res. 33 (2005) e77.
[100] M. Stoop, C.J. Leumann, Chem. Commun. 47 (2011) 7494.
[101] R.M. Franzini, E.T. Kool, J. Am. Chem. Soc. 131 (2009) 16021.
[102] Z. Ma, J.-S. Taylor, Proc. Natl. Acad. Sci. U.S.A. 97 (2000) 11159.
[103] Z. Ma, J.-S. Taylor, Bioorg. Med. Chem. 9 (2001) 2501.
[104] P.L. Carl, P.K. Chakravarty, J.A. Katzenellenbogen, J. Med. Chem. 24 (1981) 479.
[105] R. van Brakel, R.C.M. Vulders, R.J. Bokdam, H. Grüll, M.C. Robillard, Bioconjug. Chem. 19 (2008) 714.
[106] K. Gorska, A. Manicardi, S. Barluenga, N. Winssinger, Chem. Commun. 47 (2011) 4364.
[107] J. Wagner, R.A. Lerner, C.F. Barbas III, Science 270 (1995) 1797.
[108] S. Fusz, A. Eisenführ, S.G. Srivatsan, A. Heckel, M. Famulok, Chem. Biol. 12 (2005) 941.
[109] M. Oberhuber, G.F. Joyce, Angew. Chem. Int. Ed. 44 (2005) 7580.
[110] Z. Tang, A. Marx, Angew. Chem. Int. Ed. 46 (2007) 7297.
[111] J. Fan, G. Sun, C. Wan, Z. Wang, Y. Li, Chem. Commun. (2008) 3792.
[112] Y. Huang, J.M. Coull, J. Am. Chem. Soc. 130 (2008) 3238.
[113] J. Seayad, B. List, Org. Biomol. Chem. 3 (2005) 719.
[114] N. Mase, Y. Nakai, N. Ohara, H. Yoda, K. Takabe, F. Tanaka, C.F. Barbas III, J. Am. Chem. Soc. 128 (2006) 734.
[115] K. Meguellati, G. Koripelly, S. Ladame, Angew. Chem. Int. Ed. 49 (2010) 2738.
[116] G. Koripelly, K. Meguellati, S. Ladame, Bioconjug. Chem. 21 (2010) 2103.
[117] R. Huisgen, Angew. Chem. Int. Ed. Engl. 2 (1963) 565.
[118] V.V. Rostovtsev, L.G. Green, V.V. Fokin, K.B. Sharpless, Angew. Chem. Int. Ed. 41 (2002) 2596.
[119] C.W. Tornøe, C. Christensen, M. Meldal, J. Org. Chem. 67 (2002) 3057.
[120] Y. Xu, Y. Suzuki, M. Komiyama, Angew. Chem. Int. Ed. 48 (2009) 3281.
[121] T. Shiraishi, Y. Kitamura, Y. Ueno, Y. Kitade, Chem. Commun. 47 (2011) 2691.
[122] E. Jentzsch, A. Mokhir, Inorg. Chem. 48 (2009) 9593.
[123] M. Sawa, T.-L. Hsu, T. Itoh, M. Sugiyama, S.R. Hanson, P.K. Vogt, C.-H. Wong, Proc. Natl. Acad. Sci. U.S.A. 103 (2006) 12371.
[124] E.M. Sletten, C.R. Bertozzi, Org. Lett. 10 (2008) 3097.
[125] J.M. Baskin, J.A. Prescher, S.T. Laughlin, N.J. Agard, P.V. Chang, I.A. Miller, A. Lo, J.A. Codelli, C.R. Bertozzi, Proc. Natl. Acad. Sci. U.S.A. 104 (2007) 16793.
[126] X. Ning, J. Guo, M.A. Wolfert, G.-J. Boons, Angew. Chem. Int. Ed. 47 (2008) 2253.
[127] A.A. Poloukhtine, N.E. Mbua, M.A. Wolfert, G.-J. Boons, V.V. Popik, J. Am. Chem. Soc. 131 (2009) 15769.
[128] P. van Delft, N.J. Meeuwenoord, S. Hoogendoorn, J. Dinkelaar, H.S. Overkleeft, G.A. van der Marel, D.V. Filippov, Org. Lett. 12 (2010) 5486.
[129] I.S. Marks, J. Sung Kang, B.T. Jones, K.J. Landmark, A.J. Cleland, T.A. Taton, Bioconjug. Chem. 22 (2011) 1259.
[130] M. Shelbourne, X. Chen, T. Brown, A.H. El-Sagheer, Chem. Commun. 47 (2011) 6257.
[131] I. Singh, F. Heaney, Chem. Commun. 47 (2011) 2706.
[132] V. Algay, I. Singh, F. Heaney, Org. Biomol. Chem. 8 (2010) 391.
[133] K. Gutsmiedl, C.T. Wirges, V. Ehmke, T. Carell, Org. Lett. 11 (2009) 2405.
[134] K. Gutsmiedl, D. Fazio, T. Carell, Chem. Eur. J. 16 (2010) 6877.
[135] T.N. Grossmann, O. Seitz, J. Am. Chem. Soc. 128 (2006) 15596.
[136] T.N. Grossmann, L. Röglin, O. Seitz, Angew. Chem. Int. Ed. 47 (2008) 7119.
[137] R.M. Franzini, E.T. Kool, Org. Lett. 10 (2008) 2935.
[138] M. Röthlingshöfer, K. Gorska, N. Winssinger, Org. Lett. 14 (2012) 482.
[139] D.K. Prusty, A. Hermann, J. Am. Chem. Soc. 132 (2010) 12197.
[140] S. Dutta, A. Mokhir, Chem. Commun. 47 (2011) 1243.
[141] D. Arian, E. Cló, K.V. Gothelf, A. Mokhir, Chem. Eur. J. 16 (2010) 288.
[142] D. Arian, L. Kovbasyuk, A. Mokhir, Inorg. Chem. 50 (2011) 12010.
[143] S. Shimron, F. Wang, R. Orbach, I. Willner, Anal. Chem. 84 (2012) 1042.
[144] A.J. Deans, S.C. West, Nat. Rev. Cancer 11 (2011) 467, and the references therein.
[145] J. Reedijk, Chem. Commun. (1996) 801.
[146] P.M. Takahara, A.C. Rosenzweig, C.A. Frederick, S.J. Lippard, Nature 377 (1995) 649.
[147] H. Li, V.J. Broughton-Head, G. Peng, V.E.C. Powers, M.J. Ovens, K.R. Fox, T. Brown, Bioconjug. Chem. 17 (2006) 1561.
[148] R. Blasius, H. Nierengarten, M. Luhmer, J.-F. Constant, E. Defrancq, P. Dumy, A. van Dorsselaer, C. Moucheron, A. Kirsch-De Mesmaeker, Chem. Eur. J. 11 (2005) 1507.
[149] L. Ghizdavu, F. Pierard, S. Rickling, S. Aury, M. Surin, D. Beljonne, R. Lazzaroni, P. Murat, E. Defrancq, C. Moucheron, A. Kirsch-De Mesmaeker, Inorg. Chem. 48 (2009) 10988.
[150] O. Lentzen, J.-F. Constant, E. Defrancq, M. Prévost, S. Schumm, C. Moucheron, P. Dumy, A. Kirsch-De Mesmaeker, Chembiochem 4 (2003) 195.
[151] O. Lentzen, E. Defrancq, J.-F. Constant, S. Schumm, D. Garcia-Fresnadillo, C. Moucheron, P. Dumy, A. Kirsch-De Mesmaeker, J. Biol. Inorg. Chem. 9 (2004) 100.
[152] S. Le Gac, S. Rickling, P. Gerbaux, E. Defrancq, C. Moucheron, A. Kirsch-De Mesmaeker, Angew. Chem. Int. Ed. 48 (2009) 1122.
[153] H. Wang, S.E. Rokita, Angew. Chem. Int. Ed. 49 (2010) 5957.
[154] P. Wang, R. Liu, X. Wu, H. Ma, X. Cao, P. Zhou, J. Zhang, X. Weng, X.-L. Zhang, J. Qi, X. Zhou, L. Weng, J. Am. Chem. Soc. 125 (2003) 1116.
[155] S.M. Gryaznov, R. Schultz, S.K. Chaturved, R.L. Letsinger, Nucleic Acids Res. 22 (1994) 2366.
[156] M.K. Herrlein, R.L. Letsinger, Nucleic Acids Res. 22 (1994) 5076.
[157] Y. Xu, N.B. Karalkar, E.T. Kool, Nat. Biotechnol. 19 (2001) 148.
[158] S. Sando, H. Abe, E.T. Kool, J. Am. Chem. Soc. 126 (2004) 1081.
[159] D.J. Kleinbaum, E.T. Kool, Chem. Commun. 46 (2010) 8154.
[160] R.J. Lewis, P.C. Hanawalt, Nature 298 (1982) 393.
[161] J. Liu, J.-S. Taylor, Nucleic Acids Res. 26 (1998) 3300.
[162] D. Albagli, R. van Atta, P. Cheng, B. Huan, M.L. Wood, J. Am. Chem. Soc. 121 (1999) 6954.
[163] K. Fujimoto, S. Matsuda, N. Takahashi, I. Saito, J. Am. Chem. Soc. 122 (2000) 5646.
[164] S. Ogasawara, K. Fujimoto, Chembiochem 6 (2005) 1756.
[165] K. Fujimoto, S. Matsuda, M. Hayashi, I. Saito, Tetrahedron Lett. 41 (2000) 7897.
[166] K. Fujimoto, S. Matsuda, Y. Yoshimura, A. Ami, I. Saito, Chem. Commun. (2007) 2968.
[167] M. Ogino, K. Fujimoto, Angew. Chem. Int. Ed. 45 (2006) 7223.
[168] S. Ogasawara, K. Fujimoto, Angew. Chem. Int. Ed. 45 (2006) 4512.
[169] Y. Yoshimura, Y. Noguchi, H. Sato, K. Fujimoto, Chembiochem 7 (2006) 598.
[170] M. Ogino, Y. Taya, K. Fujimoto, Chem. Commun. (2008) 5996.
[171] K. Fujimoto, S. Matsuda, Y. Yoshimura, T. Matsumura, M. Hayashi, I. Saito, Chem. Commun. (2006) 3223.
[172] S. Ogasawara, K. Fujimoto, Chem. Lett. 34 (2005) 378.
[173] S. Ogasawara, T. Ami, K. Fujimoto, J. Am. Chem. Soc. 130 (2008) 10050.
[174] A. Nakamura, Y. Inoue, J. Am. Chem. Soc. 127 (2005) 5338.
[175] M. Nishijima, T. Wada, T. Mori, T.C.S. Pace, C. Bohne, Y. Inoue, J. Am. Chem. Soc. 129 (2007) 3478.
[176] C. Yang, T. Mori, Y. Origane, Y.H. Ko, N. Selvapalam, K. Kim, Y. Inoue, J. Am. Chem. Soc. 130 (2008) 8574.
[177] T. Ihara, T. Fujii, M. Mukae, Y. Kitamura, A. Jyo, J. Am. Chem. Soc. 126 (2006) 8880.
[178] M. Mukae, T. Ihara, M. Tabara, P. Arslan, A. Jyo, Supramol. Chem. 21 (2009) 292.
[179] P. Arslan, T. Ihara, M. Mukae, A. Jyo, Anal. Sci. 24 (2008) 173.
[180] M. Mukae, T. Ihara, M. Tabara, A. Jyo, Org. Biomol. Chem. 7 (2009) 1394.
[181] P. Arslan, A. Jyo, T. Ihara, Org. Biomol. Chem. 8 (2010) 4843.

International Journal of Nanomedicine

Dovepress

open access to scientific and medical research

Open Access Full Text Article

ORIGINAL RESEARCH

Biological evaluation of protein nanocapsules containing doxorubicin

This article was published in the following Dove Press journal:
International Journal of Nanomedicine
16 May 2013
Number of times this article has been viewed

Riki Toita[1,2]
Masaharu Murata[1–3]
Kana Abe[3]
Sayoko Narahara[1]
Jing Shu Piao[2]
Jeong-Hun Kang[4]
Kenoki Ohuchida[2,5]
Makoto Hashizume[1–3]

[1]Innovation Center for Medical Redox Navigation, Kyushu University, [2]Department of Advanced Medical Initiatives, Kyushu University, [3]Center for Advanced Medical Innovation, Kyushu University, Fukuoka, [4]Department of Biomedical Engineering, National Cerebral and Cardiovascular Center Research Institutes, Suita, [5]Department of Surgery and Oncology, Kyushu University, Fukuoka, Japan

Abstract: This study describes the applications of a naturally occurring small heat shock protein (Hsp) that forms a cage-like structure to act as a drug carrier. Mutant Hsp cages (HspG41C) were expressed in *Escherichia coli* by substituting glycine 41 located inside the cage with a cysteine residue to allow conjugation with a fluorophore or a drug. The HspG41C cages were taken up by various cancer cell lines, mainly through clathrin-mediated endocytosis. The cages were detected in acidic organelles (endosomes/lysosomes) for at least 48 hours, but none were detected in the mitochondria or nuclei. To generate HspG41C cages carrying doxorubicin (DOX), an anticancer agent, the HspG41C cages and DOX were conjugated using acid-labile hydrazone linkers. The release of DOX from HspG41C cages was accelerated at pH 5.0, but was negligible at pH 7.2. The cytotoxic effects of HspG41C–DOX against Suit-2 and HepG2 cells were slightly weaker than those of free DOX, but the effects were almost identical in Huh-7 cells. Considering the relatively low release of DOX from HspG41C–DOX, HspG41C–DOX exhibited comparable activity towards HepG2 and Suit-2 cells and slightly stronger cytotoxicity towards Huh-7 cells than free DOX. Hsp cages offer good biocompatibility, are easy to prepare, and are easy to modify; these properties facilitate their use as nanoplatforms in drug delivery systems and in other biomedical applications.

Keywords: anticancer activity, biomedical application, doxorubicin, drug delivery system, protein nanocapsules, small heat shock protein

Introduction

Many types of drug delivery systems, including liposomes,[1] emulsions,[2] polymers,[3,4] and proteins,[5] have been proposed to enhance the therapeutic effects and reduce the side effects of drugs. In particular, macromolecular prodrugs based on polymer–drug[6–10] and protein–drug conjugates[11,12] have received considerable attention. Unlike liposomes and polymeric micelles from which encapsulated drugs tend to be released in the bloodstream before accumulating at their target site through dissociation of thermodynamically self-assembled structures,[13,14] drug–carrier conjugates can be kept in a stable conformation if appropriate linkers are used. Although the conjugates have relatively stable characteristics, the drugs can be released from the conjugates through sensing unique cellular and subcellular environmental factors, including pH,[6–11] redox potential,[9,15] and enzyme activity,[3,12,16] and can then promote cell death. In the context of pH-sensitive prodrug systems, numerous acid-cleavable linkers, including imine,[17] acetal,[18] oxime,[19] and hydrazine,[6–11] have been reported. These linkers were generally stable at physiological conditions (pH ~7) but were hydrolyzed in the acidic environments of endosomes (pH 5–6) and lysosomes (pH 4.7).[20]

Correspondence: Masaharu Murata
Department of Advanced Medical Initiatives, Kyushu University,
3-1-1 Maidashi, Higashi-ku, Fukuoka 812-8582, Japan
Tel +81 92 642 6251
Fax +81 92 642 6252
Email m-murata@dem.med.kyushu-u.ac.jp

As a drug carrier, this study has focused on the naturally occurring small heat shock protein 16.5 (Hsp), which originated from *Methanocaldococcus jannaschii*. Hsp forms a cage-like structure with an outer diameter of 12 nm and an inner diameter of 6.5 nm through self-assembly of 24 individual monomeric proteins.[21] This Hsp cage has a monodispersed size, a well-defined structure, and can be expressed in *Escherichia coli* in a highly reproducible manner unlike other polymeric prodrugs that often require multistep reactions. In addition, the Hsp cage has eight pores with a diameter of 3 nm that allow transfer from the external to internal environment of the cage of various molecules, including fluorophores, drugs, and metal ions.[21] Therefore, Hsp cages can be fabricated with functional molecules localized on the interior and exterior of Hsp cages. Hsp cages have also been used for biomedical applications due to their advantageous biocompatibility, biodegradability, and easy fabrication through chemical/genetic strategies.[22–25] Although Hsp cages have several favorable characteristics making them suitable as drug carriers, to the best of the authors' knowledge, only a few reports have examined this possibility.[11]

In this study, an Hsp cage-based prodrug was developed. Doxorubicin (DOX) was used as a model drug because it has been clinically used to treat many cancers for more than four decades.[26,27] The interior of the native Hsp cages was first mutated to introduce cysteine residues (HspG41C), which form a complex with molecules such as fluorophores and drugs possessing maleimide groups following modification by simple thiol-maleimide chemistry. Using fluorophore (Alexa Fluor® 488)-labeled HspG41C cages (HspG41C–Alx), cellular uptake, endocytic pathways involved, and subcellular localization of HspG41C–Alx in various cancer cell lines were determined. To assess the potential applicability of Hsp cages as drug carriers, DOX was linked to Hsp cages through an acid-labile hydrazone linker by a single chemical reaction between cysteine residues inside the HspG41C cage and a maleimide group of a DOX derivative, DOX–N-(ε-maleimidocaproic acid) hydrazide, trifluoroacetic acid salt (EMCH), yielding HspG41C–DOX. The cytotoxic effects of HspG41C–DOX were then evaluated using three cancer cell lines.

Material and methods

Expression and purification of HspG41C cages

The pET21a(+) vector-encoded HspG41C mutant, in which the glycine residue at position 41 of wild-type Hsp was substituted with a cysteine residue, was prepared by polymerase chain reaction-mediated mutagenesis with appropriate primers. The success of mutagenesis was confirmed by DNA sequencing. The HspG41C mutant protein was obtained from *E. coli*, and was purified by anion exchange chromatography and size exclusion chromatography. The BL21-Gold (DE3) strain of *E. coli* (Merck KGaA, Darmstadt, Germany) was used for HspG41C expression.

E. coli containing the pET21a(+) plasmid vector were grown in 2×YT medium containing 100 μg/mL of ampicillin at 37°C. When the culture medium's optical density at 600 nm reached 0.5–0.6, the expression of the recombinant protein was induced by 1 mM isopropyl-β-$_D$-thiogalactopyranoside (Wako Pure Chemical Industries, Osaka, Japan) for 4 hours at 37°C. After collecting the cells by centrifugation, the cells were suspended in 25 mM monopotassium phosphate solution (containing 1 mM ethylenediaminetetraacetic acid and 2 mM dithiothreitol, pH 7.0) and stored at −80°C until purification. The cell suspensions were then sonicated to disrupt the cell membrane. The resulting cell lysates were centrifuged at 15,000 rpm for 30 minutes at 4°C and the supernatant was collected. Proteins were purified using a HiLoad™ 26/10 Q Sepharose™ High Performance anion exchange column (GE Healthcare, Little Chalfont, UK) and a size exclusion chromatography column (TSKgel® G3000SW; Tosoh Corporation, Tokyo, Japan). The success of purification was confirmed by 15% sodium dodecyl sulfate polyacrylamide gel electrophoresis.

Synthesis of HspG41C–Alx

To generate HspG41C complexes with fluorophores located inside the HspG41C cages, HspG41C (2.5 mg, 152 nmol cysteine residues) was reacted with Alexa Fluor 488 C_5-maleimide (0.13 mg, 182 nmol; Life Technologies, Carlsbad, CA, USA) in 0.1 M phosphate buffer (pH 7.2) for 2 hours at room temperature. The reactant was further incubated for 20 hours at 4°C. Unreacted Alexa Fluor 488 C_5-maleimide was removed by ultrafiltration using Amicon® Ultra Centrifugal Filters with a molecular weight cut-off of 100,000 (Merck).

Synthesis of maleimide hydrazone derivatives of DOX (DOX–EMCH)

DOX–EMCH was synthesized as previously reported.[9] Briefly, DOX (25 mg, 43 μmol; Wako) and EMCH (44 mg, 129 μmol; Thermo Fisher Scientific, Waltham, MA, USA) were dissolved in 12 mL methanol, and then two drops of trifluoroacetic acid were added using a Pasteur pipette. The reaction solution was stirred overnight at room temperature

in the dark. The reaction solution was then concentrated to 1 mL by evaporation and precipitated to ethyl acetate three times. The precipitate was collected by centrifugation and dried under a vacuum.

Hydrogen-1 (^{1}H) nuclear magnetic resonance (dimethyl sulfoxide-d_6, 298 K, 500 MHz), δ (ppm from tetramethylsilane): 10.29 (^{1}H, s, –N-NH-CO–), 7.93 (^{1}H, br, Ar), 7.80 (^{1}H, br, Ar), 7.67 (^{1}H, br, Ar), 6.97 (^{2}H, s, double bond of maleimide group), 4.97 (^{1}H, m, $-CH_2$-CH(–O–)$_2$ of sugar ring), 4.17 (^{2}H, m, –CH– of sugar ring), 4.04 (^{3}H, s, CH_3O-Ar), 3.36 (^{2}H, t, $-CH_2-CH_2$-N=), 2.63–3.23 (^{3}H, m, $-CH_2-$ of aliphatic ring, –CH– of sugar ring), 2.10–2.36 (^{6}H, m, $-CH_2-$ of sugar ring and aliphatic ring), 1.29–1.68 (^{6}H, m, $-CH_2-(CH_2)_3-CH_2-$), 1.17 (^{3}H, m, CH_3-CH of sugar ring).

Synthesis of DOX–EMCH-modified HspG41C (HspG41C–DOX)

HspG41C (3.2 mg, 0.19 μmol, 0.19 μmol of cysteine residue) was dissolved in phosphate buffered saline (20 mM, pH 7.2) followed by the addition of DOX–EMCH (0.6 mg, 0.78 μmol). After stirring for 2 hours, the solution was incubated for 22 hours at 4°C. Unreacted DOX–EMCH was removed by ultrafiltration as described above, which was repeated until the filtrate turned from red to clear.

Measurement of DOX release from HspG41C–DOX

HspG41C–DOX was dissolved with 0.2 M of phosphate–citrate buffer (pH 5.0) or 0.2 M of phosphate buffer (pH 7.2) to adjust the final concentration of DOX to 52 μM and final volume to 100 μL. After these HspG41C–DOX solutions were incubated at 37°C for 1, 2, or 3 days, released DOX was removed by ultracentrifugation using Amicon Ultra Centrifugal Filters with a molecular weight cut-off of 100,000 (Merck). The final volume of remaining HspG41C–DOX solution was adjusted to 100 μL by each buffer described above and then absorbance of diluted HspG41C–DOX solution was measured using ultraviolet-visible spectroscopy (V-560; JASCO, Tokyo, Japan). The percentage of released DOX from HspG41C–DOX was calculated using the following equation: percentage of DOX released = $([A_{DOX,\,0} - A_{DOX,\,X}]/A_{DOX,\,0}) \times 100$, where $A_{DOX,\,0}$ and $A_{DOX,\,X}$ were the absorbance of DOX at 495 nm at Day 0 and Day X after incubation, respectively.

Cell culture

Huh-7 cells (human hepatoma), HepG2 cells (human hepatoma), HeLa cells (human cervical carcinoma), and Suit-2 cells (human pancreatic cancer) were obtained from Japanese Collection of Research Bioresources Cell Bank (Osaka, Japan), and Hep3B cells (human hepatoma) and U87-MG cells (human glioblastoma) were obtained from American Type Culture Collection (Manassas, VA, USA). All cells were cultured in an appropriate medium containing 10% fetal bovine serum, 100 U/mL penicillin, 100 μg/mL streptomycin, and 0.25 μg/mL amphotericin-B (all from Life Technologies) in a humidified atmosphere of 5% carbon dioxide and 95% air at 37°C. Dulbecco's modified Eagle's medium was used for cultivation of Huh-7, HepG2, and U87-MG cells; Eagle's minimal essential medium containing nonessential amino acids was used for Hep3B and HeLa cells; and Roswell Park Memorial Institute 1640 was used for Suit-2 cells (all growth media were from Wako).

Fluorescence microscopic observation of HspG41C–Alx uptake

Cells were seeded on 96-well culture plates at an initial cell density of 10,000/well and were cultured for 1 day in 100 μL of the specified medium containing 10% fetal bovine serum. The final concentration of HspG41C–Alx was adjusted to 40 nM (1 μM of subunit protein) using Opti-MEM® (Life Technologies) and 100 μL of the diluted HspG41C–Alx was added to each well. After incubation for 24 hours, the medium was replaced with fresh Opti-MEM. Hoechst 33342 (Dojindo Laboratories, Kumamoto, Japan) was used to stain the nuclei. Fluorescence images were obtained using a BZ-9000 fluorescence microscope (Keyence Corporation, Osaka, Japan).

Identification of the pathway for HspG41C–Alx uptake

Suit-2 cells were harvested on poly-L-lysine-coated 48-well plates at an initial density of 50,000 cells/well and were grown overnight. Cells were treated with Dulbecco's modified Eagle's medium containing chlorpromazine (28 μM), amiloride (500 μM), and/or filipin III (15 μM) for 1 hour (all from Sigma-Aldrich, St Louis, MO, USA). Then, 84 nM of HspG41C–Alx solution containing the same concentrations of these inhibitors was added to the cells. Two hours after transfection, the cells were rinsed three times with phosphate buffered saline and lysed in lysis buffer (pH 7.5, 20 mM tris[hydroxymethyl]aminomethane hydrochloride, 2 mM ethylenediaminetetraacetic acid, and 0.05% Triton X-100). The cells lysates were transferred to black-bottomed 96-well plates and the fluorescence intensity of each sample

was measured using a microplate reader (ARVO MX 1420; PerkinElmer, Waltham, MA, USA).

Fluorescence microscopic observation of the subcellular localization of HspG41C–Alx cages and distribution of DOX

Suit-2 cells were harvested on 48-well plates at an initial density of 10,000 cells/well and were grown overnight. Then, 40 nM of HspG41C–Alx was added to the cells and the cells were cultured for 24 or 48 hours. Acidic organelles and mitochondria were stained using LysoTracker® Red DND-99 and MitoTracker® Red (Life Technologies), respectively. To assess the distribution of DOX, Suit-2 cells were harvested on 48-well plates at an initial density of 50,000 cells/well and were grown overnight. HspG41C–DOX containing 20 μM of DOX or the same concentration of free DOX was added to the cells, which were incubated for 24 or 48 hours. Fluorescence images were obtained using the BZ-9000 fluorescence microscope.

Evaluation of HspG41C cytotoxicity

Cells were harvested on white-bottomed 96-well plates at an initial cell density of 10,000 cells/well and were grown overnight. Then, 100 μL of HspG41C dissolved in Opti-MEM (1–100 μg/mL) was added to the cells, which were then incubated for 24 hours. Cell viability was measured using a CellTiter-Glo® luminescent cell viability assay kit (Promega Corporation, Madison, WI, USA). Luminescence intensity was measured using the ARVO MX 1420 microplate reader.

Evaluation of cytotoxicity of HspG41C–DOX to cells

The cells were harvested on white-bottomed 96-well plates at an initial cell density of 10,000 cells/well and were grown overnight. Then, 100 μL of HspG41C–DOX dissolved in Opti-MEM (containing 0.3–30 μM of DOX) was added to the cells. After incubation for 24, 48, or 72 hours, cell viability was measured as described above. Half maximal inhibitory concentration (IC_{50}) factors were calculated using Prism® sigmoidal dose response software (GraphPad Prism 6; GraphPad Software, Inc, La Jolla, CA, USA).

Results and discussion

Characterization of HspG41C

Hsp is a naturally occurring protein that forms a cage structure with an external diameter of 12 nm and an internal diameter of 6.5 nm through self-assembly of 24 individual monomeric proteins.[21] To introduce the conjugation sites of chemical agents such as fluorophores and drugs, a mutant Hsp cage (HspG41C) was developed by genetically substituting glycine 41, within the interior of the Hsp cage, with cysteine. HspG41C cages were obtained from *E. coli*, and were purified by anion exchange chromatography and size exclusion chromatography. The resulting size exclusion chromatography profile and sodium dodecyl sulfate polyacrylamide gel electrophoresis analysis revealed that HspG41C was successfully obtained (Figure 1A). Dynamic light scattering measurements confirmed that the resulting HspG41C had a diameter of ~12 nm, which is consistent with previous results (Figure 1B).[21] In addition, HspG41C at concentrations of 1–100 μg/mL showed no cytotoxicity against HepG2 cells or Suit-2 cells (Figure 2), indicating that HspG41C is a biocompatible protein with favorable

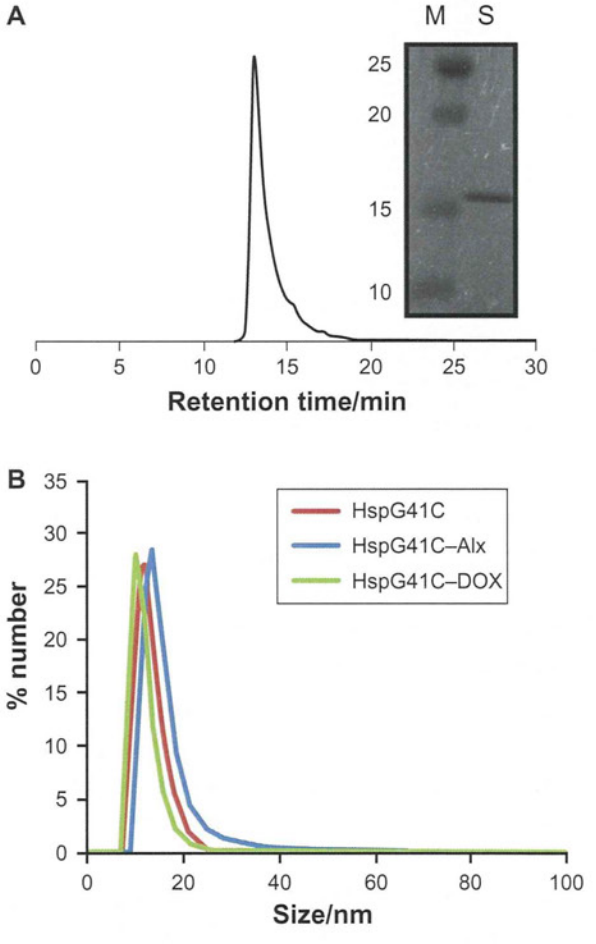

Figure 1 (**A**) Size exclusion chromatography profile of HspG41C. The picture to the right shows a typical sodium dodecyl sulfate polyacrylamide gel electrophoresis blot of HspG41C purified by ion exchange chromatography and size exclusion chromatography. (**B**) Size distribution of HspG41C, HspG41C–Alx, and HspG41C–DOX in phosphate buffered saline.

Abbreviations: HspG41C, mutant heat shock protein cage; HspG41C–Alx, fluorophore (Alexa Fluor® 488)-labeled HspG41C cage; HspG41C–DOX, HspG41C–cage carrying doxorubicin; M, marker; S, monomeric HspG41C.

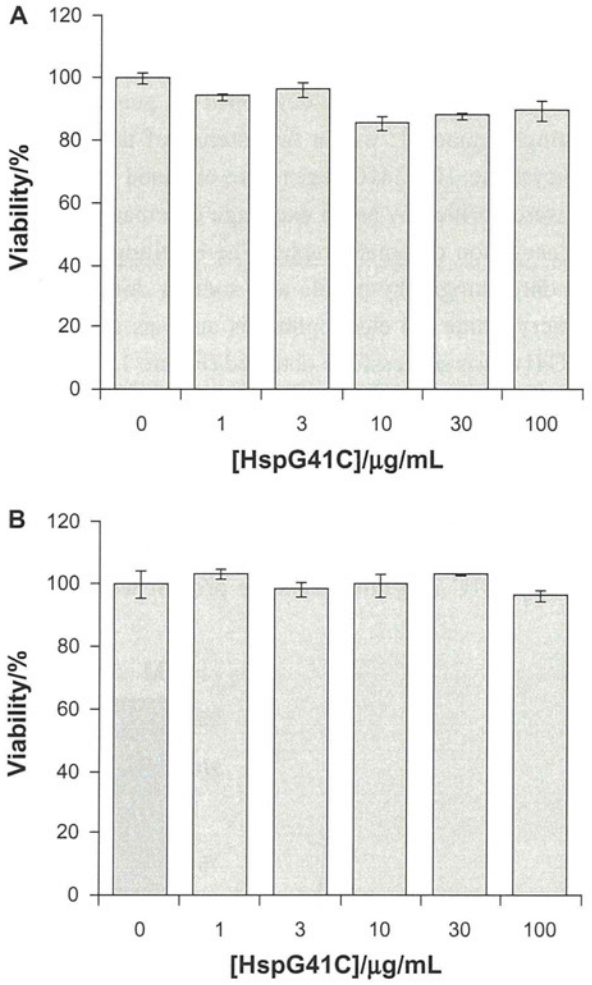

Figure 2 Cytotoxicity assay of HspG41C against (**A**) Suit-2 cells (human pancreatic cancer cells) and (**B**) HepG2 cells (human hepatocellular carcinoma cells).
Note: Data represents mean ± standard error of the mean (n = 3).
Abbreviation: HspG41C, mutant heat shock protein cage.

characteristics and is useful as a drug delivery system and in other biomedical applications.

Cellular uptake of HspG41C by various cell lines

To examine whether the HspG41C cages could be taken up by the cells, HspG41C–Alx were prepared by Michael addition reaction between Alexa Fluor 488 maleimide and the unique cysteine residue of HspG41C. The resulting HspG41C–Alx had a comparable size distribution to that of unmodified HspG41C (Figure 1B). HspG41C–Alx was added to cultures of HepG2, Hep3B, Huh-7, Suit-2, U87-MG, and HeLa cells. HspG41C–Alx uptake was observed by fluorescence microscopy 24 hours later. Green fluorescence corresponding to HspG41C–Alx was detected in each of the cell lines (Figure 3), confirming that HspG41C-Alx could be taken up by various cell types.

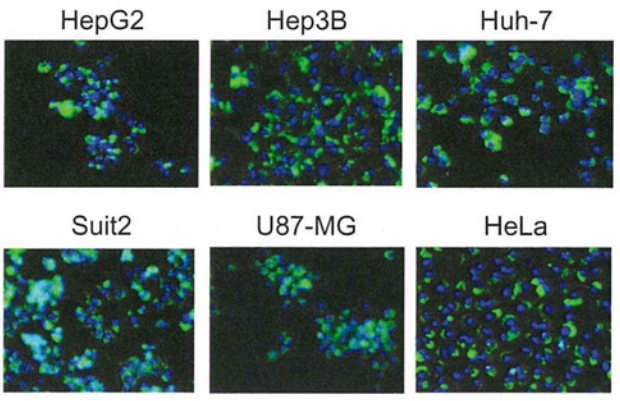

Figure 3 Uptake of HspG41C–Alx cages by cancer cell lines.
Notes: Cells were incubated with 40 nM of HspG41C (1 μM of protein monomer unit) for 24 hours and observed by fluorescence microscopy. Green indicates HspG41C–Alx cages; blue indicates the nuclei.
Abbreviations: HspG41C, mutant heat shock protein cage; HspG41C–Alx, fluorophore (Alexa Fluor® 488)-labeled HspG41C cage.

Endocytic mechanism and subcellular localization of HspG41C cages

The HspG41C nanoparticles were mostly internalized by endocytosis. The endocytic pathways are broadly classified into four groups, namely clathrin-mediated endocytosis, caveolae-mediated endocytosis, macropinocytosis, and clathrin- and caveolae-independent endocyotosis.[28] Therefore, to determine the endocytic pathway involved in HspG41C internalization, the following compounds that inhibit specific endocytic pathways were used (Figure 4): chlorpromazine, which inhibits clathrin-mediated endocytosis;[29] amiloride, which inhibits macropinocytosis;[30] and filipin III, which inhibits caveolae-mediated endocytosis.[31] Pretreatment of Suit-2 cells with amiloride and filipin III decreased the cellular uptake of HspG41C by 8% and 19%, respectively, compared with untreated cells. On the other hand, pretreatment with chlorpromazine elicited a much greater decrease (42%) in the uptake of HspG41C. Pretreatment with all three compounds simultaneously elicited a similar decrease (52%) in the uptake of HspG41C to that of chlorpromazine alone. These results indicate that main uptake pathway of HspG41C was clathrin-mediated endocytosis.

Nanoparticles that are taken up by clathrin-mediated endocytosis usually enter endosomal vesicles and are then translocated to lysosomes with more acid pH (5.0–6.5) compared with the cytosol (pH 7.2).[20,28] Some nanoparticles escape these acidic organelles and accumulate in the mitochondria and nuclei. Therefore, to determine the subcellular localization of HspG41C, Suit-2 cells were incubated with HspG41C–Alx for 24 or 48 hours and the colocalization of HspG41C–Alx with specific organelles

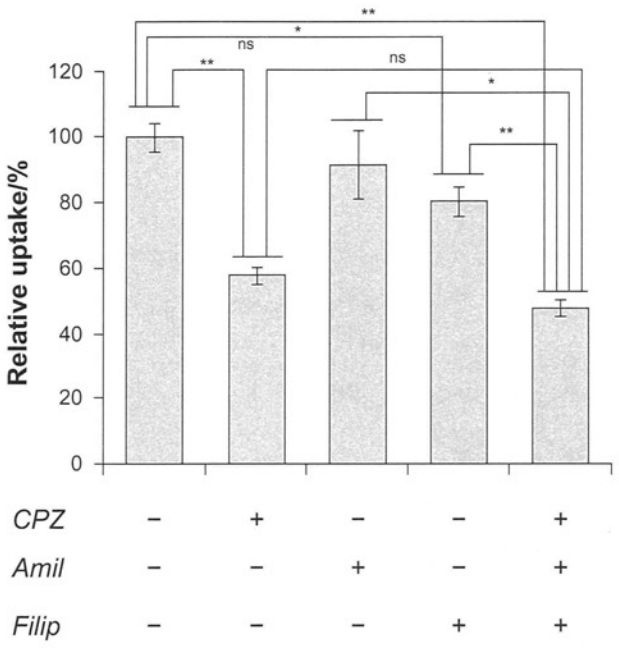

Figure 4 Inhibition of cellular uptake of HspG41C–Alx cages by three types of endocytosis inhibitors.

Notes: Uptake of HspG41C–Alx cages was measured as the fluorescence intensity after incubation with HspG41C–Alx cages for 2 hours. $*P < 0.05$; $**P < 0.01$; data represents mean ± standard error of the mean (n = 3).

Abbreviations: Amil, amiloride; CPZ, chlorpromazine; Filip, filipin III; HspG41C, mutant heat shock protein cage; HspG41C–Alx, fluorophore (Alexa Fluor® 488)-labeled HspG41C cage; ns, not significant.

(acidic organelles, mitochondria, and nuclei) was observed by fluorescence microscopy. The fluorescence images showed that HspG41C–Alx was mainly localized in the endosomes and/or lysosomes at 24 hours based on the merged fluorescence of HspG41C–Alx and LysoTracker (shown in yellow; Figure 5A). After 48 hours, most of the HspG41C–Alx remained in the endosomes/lysosomes. Very slight colocalization of HspG41C–Alx in mitochondria (stained with MitoTracker Red) was found at 48 hours because accumulation of HspG41C–Alx in mitochondria required endosomal escape (Figure 5B).

Synthesis of HspG41C–DOX and DOX release

Next, HspG41C–DOX was prepared as a drug delivery system by covalently binding a DOX derivative (DOX–EMCH; Figure 6) by acid-labile hydrazone binding in the interior of HspG41C cages. This was achieved by simple Michael addition reactions between a maleimide group of DOX–EMCH and the unique cysteine residue of HspG41C. After conjugation, 20 molecules of DOX–EMCH were covalently bound to one HspG41C–DOX cage based on the absorbance of DOX–EMCH ($\varepsilon_{495} = 8030\ M^{-1}\ cm^{-1}$). No obvious change

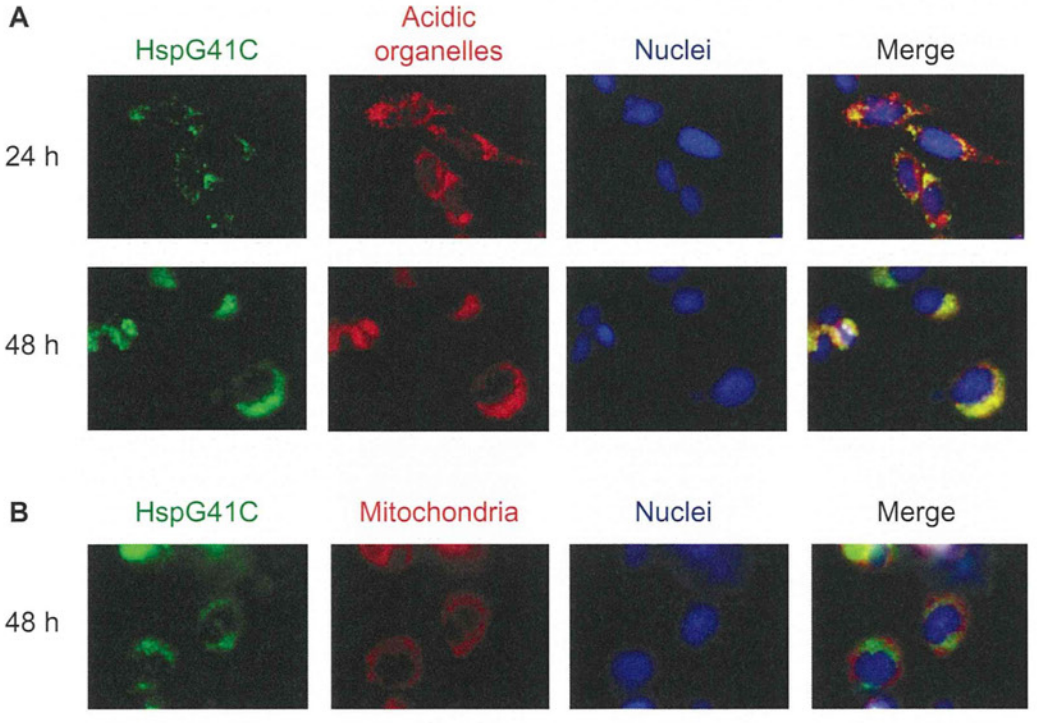

Figure 5 Fluorescence microscopic observation of the subcellular localization of HspG41C cages. Suit-2 cells were incubated with 40 nM of HspG41C–Alx for 24 or 48 hours and observed by fluorescence microscopy. (**A**) Acidic organelles (endosomes/lysosomes) and (**B**) mitochondria were stained with LysoTracker® Red and MitoTracker® Red, respectively (both are shown in red). Nuclei (blue) were stained by Hoechst 33342.

Abbreviations: HspG41C, mutant heat shock protein cage; HspG41C–Alx, fluorophore (Alexa Fluor® 488)-labeled HspG41C cage.

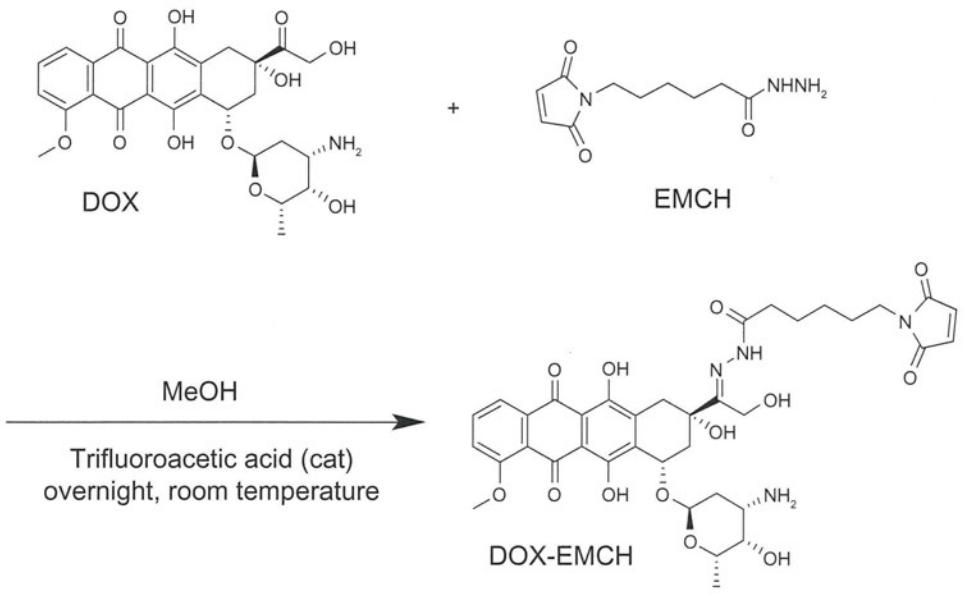

Figure 6 Synthetic scheme of DOX–EMCH.
Abbreviations: DOX, doxorubicin; EMCH, N-(ε-maleimidocaproic acid) hydrazide, trifluoroacetic acid salt; MeOH, methanol.

in size distribution of HspG41C–DOX was detected when compared with unmodified HspG41C (Figure 1B). As shown in Figure 7, approximately 60% of conjugated DOX was released from HspG41C–DOX 2 days after incubating at pH 5.0 and the amount of DOX released was almost comparable between samples incubated for 2 days and 3 days. By contrast, a much smaller amount of DOX (~10%) was released after incubating at pH 7.2 for 3 days. These results indicate that the release of DOX from HspG41C is accelerated in acidic environments, as in endosomes/lysosomes.

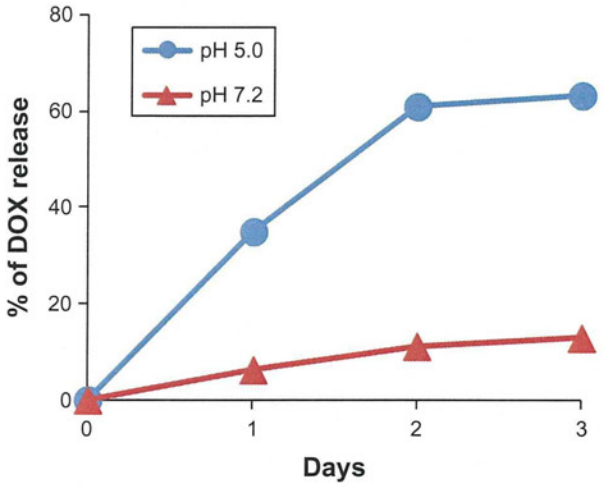

Figure 7 Time course of DOX release from HspG41C–DOX at pH of 5.0 and 7.2.
Note: Data represents mean ± standard error of the mean (n = 3).
Abbreviations: DOX, doxorubicin; HspG41C, mutant heat shock protein cage; HspG41C–DOX, HspG41C cage carrying doxorubicin.

Evaluation of HspG41C–DOX cytotoxicity

Cytotoxic assays of HspG41C-DOX against Suit-2, HepG2, and Huh-7 cancer cell lines were then performed. HspG41C–DOX and free DOX at concentrations of 0.3–30 μM were added to the cells and the number of viable cells was measured using a CellTiter-Glo kit at the specified times (24–72 hours) (Figure S1). The IC_{50} values of HspG41C–DOX and free DOX were then determined (Table 1). The morphology of Suit-2 cells changed from a "sharp" appearance (Figure 8A) to a "round" appearance at 24 hours after treatment with free DOX (Figure 8B) and HspG41C–DOX

Table 1 Half maximal inhibitory concentration values of a mutant heat shock protein cage (HspG41C) carrying doxorubicin and free doxorubicin

Cells	Exposure time (hours)	IC_{50} (μM)	
		HspG41C–DOX	Free DOX
Huh-7 (hepatoma)	24	16	>30
	48	5.5	10
	72	1.1	1.9
HepG2 (hepatoma)	24	20	4.5
	48	7.8	1.2
	72	4.8	1.2
Suit-2 (pancreatic cancer)	24	>30	>30
	48	4.5	1.6
	72	2.7	1.4

Abbreviations: DOX, doxorubicin; HspG41C–DOX, mutant heat shock protein cage (HspG41C) carrying doxorubicin; IC_{50}, half maximal inhibitory concentration.

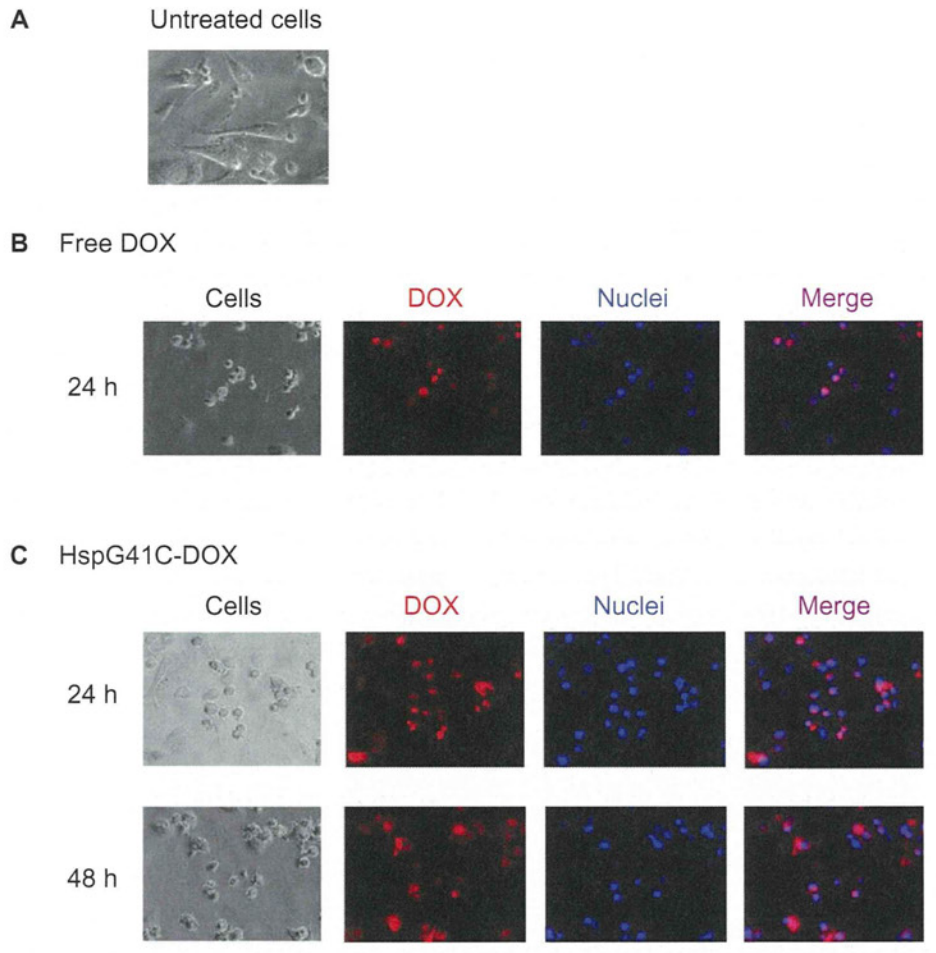

Figure 8 Fluorescence microscopic analysis of the subcellular localization of DOX in Suit-2 cells. (**A**) Untreated Suit-2 cells. Cellular distribution of (**B**) free DOX and (**C**) HspG41C–DOX.
Notes: Red indicates DOX; blue indicates the nuclei.
Abbreviations: DOX, doxorubicin; HspG41C, mutant heat shock protein cage; HspG41C–DOX, HspG41C cage carrying doxorubicin.

(Figure 8C), predominantly as a result of cell death. The IC_{50} values of HspG41C–DOX in Suit-2 and HepG2 cells were three to four times higher than those of free DOX. In Huh-7 cells, the IC_{50} values of both DOX formations were almost identical.

It was hypothesized that the weaker cytotoxicity of HspG41C–DOX compared with free DOX was caused by differences in subcellular localization between both formations of DOX because DOX can induce cell death in various ways including inhibition of DNA topoisomerase II, DNA binding, DNA intercalation, and inhibition of DNA replication[26,27] as well as mitochondrial malfunction through nonspecific oxidative damage towards mitochondrial inner and outer membranes and interactions with mitochondrial enzymes and DNA.[26] As shown in Figure 8B and C, both formations of DOX were predominantly found in the cytoplasm and nuclei. It was then further investigated whether released DOX reached the mitochondria using MitoTracker Green, a commercially available staining reagent for mitochondria. Unfortunately, after treatment with HspG41C–DOX and DOX, mitochondria were difficult to stain maybe due to the death of cells (data not shown). Therefore, it was difficult to clarify the reason why HspG41C–DOX showed lower cytotoxicity than free DOX based on the differences in subcellular localization. Another possible reason for weaker cytotoxicity of HspG41C–DOX is considered to be the relatively low amount of DOX released from HspG41C–DOX. As shown in Figure 7, ~60% of DOX was released from HspG41C–DOX at 3 days after incubation in buffered solution with pH 5.0 (simulating pH of the late endosome), while only ~10% of DOX was released when incubated in buffered solution with pH 7.2 (simulating pH of the cytoplasm). These results showed that most of DOX can be released from HspG41C–DOX in acidic organelles but not in cytoplasm, and DOX cannot be completely released at 3 days after incubation at pH 5.0. Therefore, to increase the cytotoxicity of HspG41C–DOX, the hydrazone linkers should

be replaced with more effective acid-cleavable linkers to increase the amount of DOX released from HspG41C–DOX. In a previous report, poly($_L$-lactic acid)-poly(ethylene glycol) diblock copolymers linked with DOX using a cis-aconityl linker enabled quicker release of DOX at pH 5 compared with the use of a hydrazone linker, whereas the cis-acotinyl bond was almost completely stable at pH 7.[10] Therefore, substitution of a hydrazone linker with a cis-acotinyl linker may be a promising approach to enhance the cytotoxicity effect of the HspG41C–DOX cage used in this study.

Many types of DOX conjugates connecting through hydrazone linkers (eg, polymer, polyamino acid, and protein conjugates) were reported and these typically showed dozens of times lower cytotoxicity than that of free DOX in vitro.[32,33] Therefore, the HspG41C–DOX conjugate was a slightly superior system in vitro compared with others. Interestingly, in contrast to in vitro experiments, DOX conjugates exhibited greater inhibition of tumor growth without severe side effects in healthy tissue when applied to tumor-xenografted animal models.[32,33] Therefore, to fully assess the therapeutic effect and side effects, additional in vivo experiments using HspG41C–DOX are required.

Future plans

As described above, a major drawback of the present HspG41C–DOX was lower cytotoxicity than free DOX possibly due to slow release of DOX from HspG41C–DOX. Therefore, an attempt to overcome this problem through exchanging the hydrazone linkers to more effective acid cleavable linkers (eg, cis-aconityl linkers) will be made. Also, for in vivo application, specific drug delivery to target cells was very important in order to avoid any undesirable side effects. An advantage of Hsp cages is that the peptide ligand can be modified by the chemical/genetic method,[22,23] enabling the delivery of cytotoxic reagents to specific cells. It was previously reported that Hsp cages could specifically target human hepatoma cells after binding human hepatoma binding peptides (SP94 peptides) to the surface of the Hsp cages using poly(ethylene glycol) linkers. The resulting HspSP94 cage was specifically taken up by human hepatoma cells but not by normal liver cells.[22] Accordingly, an attempt will be made to modify the peptide to Hsp cages and changing the linker between Hsp and DOX to a more acid-responsive linker, which will enhance the usefulness of Hsp cages in a drug delivery system.

Conclusion

It has been shown that genetically engineered HspG41C cages provide a useful drug delivery system of DOX to various cancer cell lines. The HspG41C cages were taken up by various cell lines, mainly through clathrin-mediated endocytosis, without cytotoxic effects, and were localized in acidic organelles for at least 48 hours. Cysteine residues inside the HspG41C cages can be chemically modified to bind to various drugs and fluorophores. As a model drug delivery system, HspG41C–DOX cages were taken up by cells and DOX was released from HspG41C–DOX following cleavage of the hydrazone bonds between HspG41C and DOX in acidic organelles, leading to cell death. Taking into account the low release rate of DOX from HspG41C, HspG41C–DOX exhibited comparable activity towards HepG2 and Suit-2 cells and slightly stronger cytotoxicity towards Huh-7 cells than free DOX. Hsp cages offer good biocompatibility, are easy to prepare, and are easy to modify; these properties facilitate their use as nanoplatforms for drug delivery systems and in other biomedical applications. Further refinements of HspG41C–DOX are still required, including changing the linker between DOX and the Hsp cages, and improving cell specificity.

Acknowledgments

This work was financially supported by a Health Labor Sciences Research Grant (Research on Publicly Essential Drugs and Medical Devices) from the Ministry of Health, Labor, and Welfare of Japan, and the Special Coordination Funds for Promoting Science and Technology of Japan (SCF funding program "Innovation Center for Medical Redox Navigation"), and a Grant-in-Aid for Research Activity Start-up (number 23800045) from the Ministry of Education, Culture, Sports, Science, and Technology of Japan.

Disclosure

The authors report no conflicts of interest in this work.

References

1. Ceh B, Wintherhalter M, Frederik PM, Vallner JJ, Lasic DD. Stealth® liposomes: from theory to product. *Adv Drug Deliv Rev*. 1997; 24(2–3):165–177.
2. Tahara Y, Kaneko T, Toita R, et al. A novel double-coating carrier produced by solid-in-oil and solid-in-water nanodispersion technology for delivery of genes and proteins in cells. *J Control Release*. 2012;161(3): 713–721.
3. Toita R, Kang JH, Tomiyama T, et al. Gene carrier showing all-or-none response to cancer cell signaling. *J Am Chem Soc*. 2012;134(37): 15410–15417.
4. Cover NF, Lai-Yuen S, Parsons AK, Kumar A. Synergetic effects of doxycycline-loaded chitosan nanoparticles for improving drug delivery and efficacy. *Int J Nanomedicine*. 2012;7:2411–2419.
5. Elsadek B, Kratz F. Impact of albumin on drug delivery – new applications on the horizon. *J Control Release*. 2012;157(1):4–28.

6. Du JZ, Du XJ, Mao CQ, Wang J. Tailor-made dual pH-sensitive polymer–doxorubicin nanoparticles for efficient anticancer drug delivery. *J Am Chem Soc*. 2011;133(44):17560–17563.
7. Zhou L, Cheng R, Tao H, et al. Endosomal pH-activatable poly(ethylene oxide)-graft-doxorubicin prodrugs: synthesis, drug release, and biodistribution in tumor-bearing mice. *Biomacromolecules*. 2011;12(5):1460–1467.
8. Bae Y, Fukushima S, Harada A, Kataoka K. Design of environment-sensitive supramolecular assemblies for intracellular drug delivery: polymeric micelles that are responsive to intracellular pH change. *Angew Chem Int Ed*. 2003;42(38):4640–4643.
9. Jia Z, Wong L, Davis TP, Bulmus V. One-pot conversion of RAFT-generated multifunctional block copolymers of HPMA to doxorubicin conjugated acid- and reductant-sensitive crosslinked micelles. *Biomacromolecules*. 2008;9(11):3106–3113.
10. Yoo HS, Lee EA, Park TG. Doxorubicin-conjugated biodegradable polymeric micelles having acid-cleavable linkages. *J Control Release*. 2002;82(1):17–27.
11. Flenniken ML, Liepold LO, Crowley BE, Willits DA, Young MJ, Douglas T. Selective attachment and release of a chemotherapeutic agent from the interior of a protein cage architecture. *Chem Commun (Camb)*. 2005;(4):447–449.
12. Mansour AM, Drevs J, Esser N, et al. A new approach for the treatment of malignant melanoma: enhanced antitumor efficacy of an albumin-binding doxorubicin prodrug that is cleaved by matrix metalloproteinase 2. *Cancer Res*. 2003;63(14):4062–4066.
13. Chen H, Kim S, He W, et al. Fast release of lipophilic agents from circulating PEG-PDLLA micelles revealed by in vivo Forster resonance energy transfer imaging. *Langmuir*. 2008;24(10):5213–5217.
14. Jiwpanich S, Ryu JH, Bickerton S, Thayumanavan S. Noncovalent encapsulation stabilities in supramolecular nanoassemblies. *J Am Chem Soc*. 2010;132(31):10683–10685.
15. Santra S, Kaittanis C, Santiesteban OJ, Perez JM. Cell-specific, activatable, and theranostic prodrug for dual-targeted cancer imaging and therapy. *J Am Chem Soc*. 2011;133(41):16680–16688.
16. Denmeade SR, Nagy A, Gao J, Lilja H, Schally AV, Isaacs JT. Enzymatic activation of a doxorubicin-peptide prodrug by prostate-specific antigen. *Cancer Res*. 1998;58(12):2537–2540.
17. Gillies ER, Frechet JM. pH-responsive copolymer assemblies for controlled release of doxorubicin. *Bioconjug Chem*. 2005;16(2):361–368.
18. Gillies ER, Frechet JM. A new approach towards acid sensitive copolymer micelles for drug delivery. *Chem Commun (Camb)*. 2003;14:1640–1641.
19. Jin Y, Song L, Su Y, et al. Oxime linkage: a robust tool for the design of pH-sensitive polymeric drug carriers. *Biomacromolecules*. 2011;12(10):3460–3468.
20. Casey JR, Grinstein S, Orlowski J. Sensors and regulators of intracellular pH. *Nat Rev Mol Cell Biol*. 2010;11(1):50–61.
21. Kim KK, Kim R, Kim SH. Crystal structure of a small heat-shock protein. *Nature*. 1998;394(6693):595–599.
22. Toita R, Murata M, Tabata S, et al. Development of human hepatocellular carcinoma cell-targeted protein cages. *Bioconjug Chem*. 2012;23(7):1494–1501.
23. Murata M, Narahara S, Umezaki K, et al. Liver cell specific targeting by the preS1 domain of hepatitis B virus surface antigen displayed on protein nanocages. *Int J Nanomedicine*. 2012;7:4353–4362.
24. Sao K, Murata M, Umezaki K, et al. Molecular design of protein-based nanocapsules for stimulus-responsive characteristics. *Bioorg Med Chem*. 2009;17(1):85–93.
25. Sao K, Murata M, Fujisaki Y, et al. A novel protease activity assay using a protease-responsive chaperone protein. *Biochem Biophys Res Commun*. 2009;383(3):293–297.
26. Jung K, Reszka R. Mitochondria as subcellular targets for clinically useful anthracyclines. *Adv Drug Deliv Rev*. 2001;49(1–2):87–105.
27. Kizek R, Adam V, Hrabeta J, et al. Anthracyclines and ellipticines as DNA-damaging anticancer drugs: recent advances. *Pharmacol Ther*. 2012;133(1):26–39.
28. Sahay G, Alakhova DY, Kabanov AV. Endocytosis of nanomedicines. *J Control Release*. 2010;145(3):182–195.
29. Wang LH, Rothberg KG, Anderson RG. Mis-assembly of clathrin lattices on endosomes reveals a regulatory switch for coated pit formation. *J Cell Biol*. 1993;123(5):1107–1117.
30. Hewlett LJ, Prescott AR, Watts C. The coated pit and macropinocytic pathways serve distinct endosome populations. *J Cell Biol*. 1994;124(5):689–703.
31. Lamaze C, Schmid SL. The emergence of clathrin-independent pinocytic pathways. *Curr Opin Cell Biol*. 1995;7(4):573–580.
32. Bae Y, Nishiyama N, Fukushima S, Koyama H, Matsumura Y, Kataoka K. Preparation and biological characterization of polymeric micelle drug carriers with intracellular pH-triggered drug release property: tumor permeability, controlled subcellular drug distribution, and enhanced in vivo antitumor efficacy. *Bioconjug Chem*. 2005;16(1):122–130.
33. Kratz F, Warnecke A, Scheuermann K, et al. Probing the cystein-34 position of endogenous serum albumin with thiol-binding doxorubicin derivatives. Improved efficacy of an acid-sensitive doxorubicin derivative with specific albumin-binding properties compared to that of the parent compound. *J Med Chem*. 2002;45(25):5523–5533.

Supplementary figure

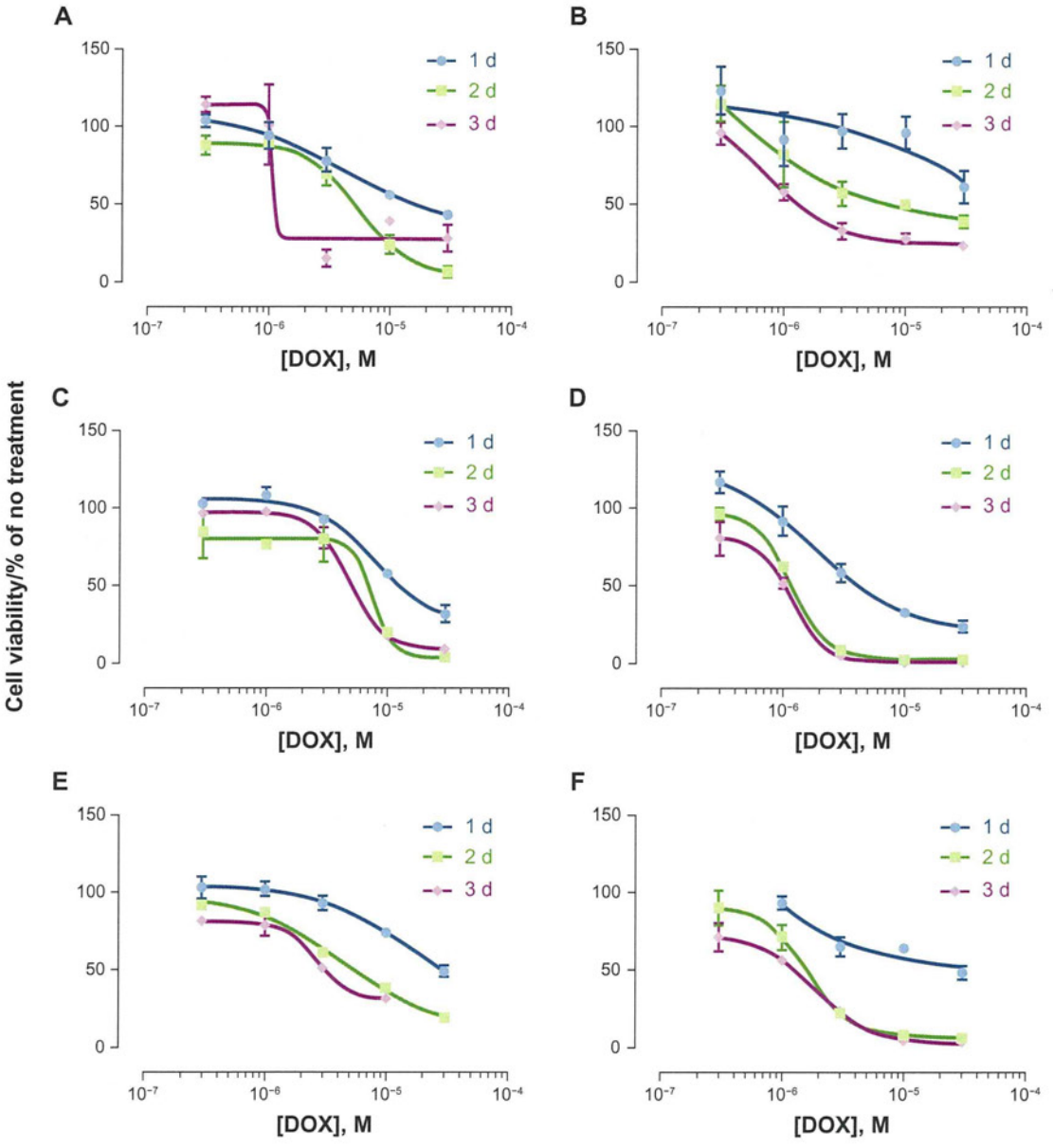

Figure S1 Cytotoxicity of (**A**, **C** and **E**) HspG41C–DOX and (**B**, **D** and **F**) free DOX.
Notes: One to three days after adding HspG41C–DOX and free DOX (concentrations of DOX were 0.3–30 μM) to (**A** and **B**) Huh-7 cells, (**C** and **D**) HepG2 cells, (**E** and **F**) and Suit-2 cells, cell viability was measured using CellTiter-Glo® kit. Data represents mean ± standard error of the mean (n = 3).
Abbreviations: DOX, doxorubicin; HspG41C, mutant heat shock protein cage; HspG41C–DOX, HspG41C cage carrying doxorubicin.

ChemComm

RSC Publishing

COMMUNICATION

Versatile allosteric molecular devices based on reversible formation of luminous lanthanide complexes†

Cite this: *Chem. Commun.*, 2013, **49**, 285

Received 26th September 2012, Accepted 13th November 2012

DOI: 10.1039/c2cc36979f

www.rsc.org/chemcomm

Yusuke Kitamura,*[ab] Shikinari Yamamoto,[a] Yuka Osawa,[a] Hirotaka Matsuura[a] and Toshihiro Ihara*[ab]

A versatile molecular device (lanthanide-complex molecular beacon; LCMB) was prepared by tethering ethylenediaminetetraacetic acid to the 5′-end and 1,10-phenanthroline to the 3′-end of stem–loop structured DNA as metal-capturing and sensitizer moieties, respectively. The emission from LCMB responded to the target molecule through the reversible structural change.

For several years, we have been engaged in the development of a system for gene analysis through cooperative action between probes.[1] In a series of studies, we showed that the hybridization of oligodeoxyribonucleotide (ODN) conjugates bearing a metal chelator on their terminus was efficiently controlled by a metal ion as an allosteric effector. This work suggested that the general concept of "metal-ion-directed cooperative recognition"[2] could be applied to the split-probing of specific genes,[3] using luminescent lanthanides as metal ions. Metal-centered luminescence from complexes of trivalent lanthanide (Ln(III)) ions has been widely exploited in bioassays.[4] The long luminescence (up to the millisecond range) lifetime permits the use of time-gating techniques to eliminate the short-lived (the nanosecond range) fluorescence background present in biological samples. In addition, large Stokes shifts minimize crosstalk between excitation light and emission signals, and narrow emission bands in the NIR to UV range enable us to perform multicolor assays.[5] The utility of this concept was demonstrated using two DNA conjugates carrying ethylenediaminetetraacetic acid (EDTA) and 1,10-phenanthroline (phen) on each of their termini to function as a capturing and a sensitizer moiety, respectively, for Ln(III). Since the sequences of the two probes are designed to be complementary to the adjacent sites of the target, both auxiliary units of the two probes face each other, providing a microenvironment to accommodate Ln(III).[1d–g,6] Luminous Ln(III) complexes were obtained only in the presence of the fully matched target. The emission intensity was very sensitive to one-base displacement on the target sequence.[1d–g]

We now report a molecular device consisting of a lanthanide complex and a stem–loop-structured ODN. The molecular device, called a lanthanide-complex molecular beacon (LCMB), was prepared by the introduction of EDTA at the 5′-end and phen at the 3′-end. In the stem–loop structure, the modified auxiliary units on both ends of the ODN are placed in close proximity, providing a microenvironment to accommodate Ln(III) (Fig. 1). The luminescence from the Ln(III) complex is therefore expected to depend on the whole structural conformation of the LCMB. Here, we show a versatile principle for biosensing, based on time-resolved fluorometry, using the reversible conformational changes of the LCMB in response to analytes.

To prepare LCMBs, EDTA and phen were covalently modified at each aminated end of ODNs by coupling of the corresponding anhydrous derivative and an active ester, respectively (see details in the ESI†). The stability constants of phen–Ln(III) are

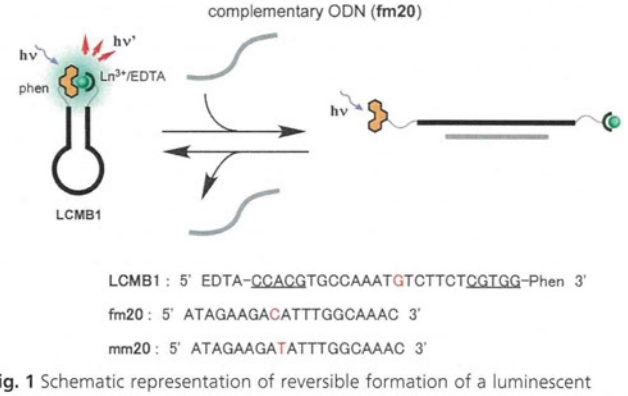

Fig. 1 Schematic representation of reversible formation of a luminescent lanthanide complex, and the sequence of the lanthanide-complex molecular beacon (**LCMB1**). The underlined region indicates the complementary bases for stem duplex formation.

[a] *Department of Applied Chemistry and Biochemistry, Kumamoto University, 2-39-1 Kurokami, Chuo-ku, Kumamoto 860-8555, Japan. E-mail: ykita@kumamoto-u.ac.jp, toshi@chem.kumamoto-u.ac.jp; Fax: +81 96 342 3873; Tel: +81 96 342 3873*

[b] *CREST, Japan Science and Technology Agency, 7 Gobancho, Chiyoda-ku, Tokyo 102-0076, Japan*

† Electronic supplementary information (ESI) available: Detailed information on the synthesis of molecular devices, optimized linker length for molecular devices and the calibration curve of emission intensities as a function of the concentration of ATP. See DOI: 10.1039/c2cc36979f

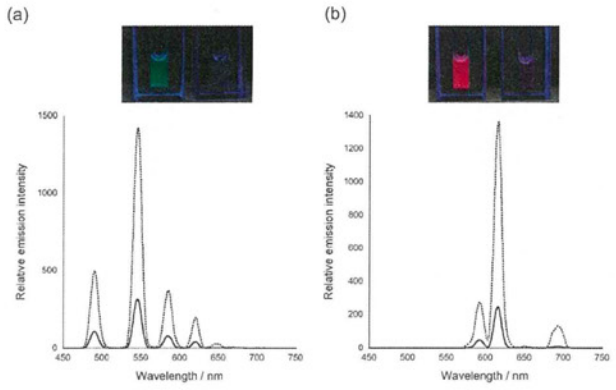

Fig. 2 Time-gated emission spectra (λ_{ex} = 280 nm) of solutions containing **LCMB1** with (solid curve) and without (dashed curve) **fm20** in the presence of (a) Tb(III) or (b) Eu(III). Measurements were carried out in buffered solution (10 mM HEPES containing 50 mM NaCl, pH 7.0) at 0 °C. Concentrations of **LCMB1** and Ln(III) were 1.0 μM, and that of **fm20** was 5.0 μM. Delay time: 50 μs; gate time: 2.0 ms. Inset: luminescence images of solutions of Ln(III)–**LCMB1** (left) and Ln(III)–**LCMB1** + **fm20** (right) at 5 °C. Excitation source: low-pressure mercury lamp (6 W).

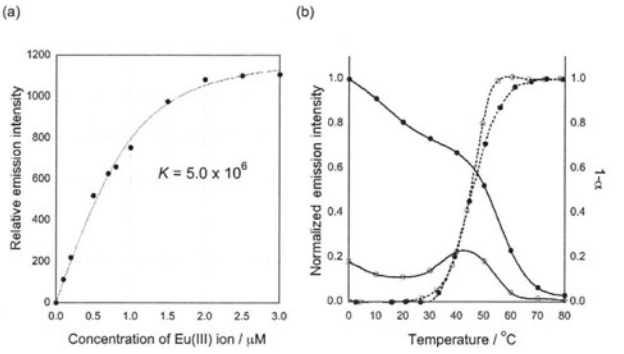

Fig. 3 (a) Emission titration curve for **LCMB1** (1.0 μM) with Eu(III) ions. (b) Temperature-dependent emission intensities (solid curves) and normalized UV melting curves (dashed curves) of Eu(III)–**LCMB1** (filled circles) and Eu(III)–**LCMB1**/**fm20** (open circles). α is the fraction of single strands in the duplex state. The measurements were carried out in the same buffer solution as used in the measurements of Fig. 2.

too low for complex formation under the experimental conditions without the assistance of the EDTA attached to the other end. Therefore, unlike the case of a traditional molecular beacon (MB), the emission from an LCMB is expected to occur only in its closed (stem–loop) conformation.[7]

First, the specificity of the luminescence response of the system to the target DNA was examined using **LCMB1** (Fig. 1). As shown in Fig. 2a and b, the characteristic emissions of Tb(III) and Eu(III) ions were clearly observed for solutions containing **LCMB1** and an equimolar amount of the corresponding Ln(III). An extremely low background signal with a high signal-to-noise ratio was observed using a time-resolved technique (quantum yields: $\phi_{Tb(III)}$ = 0.17, $\phi_{Eu(III)}$ = 0.10).‡ The emission was identified, even by the naked eye, as green and red light for Tb(III) and Eu(III), respectively. These results indicated that the two auxiliary units that gathered on top of the stem–loop structure of **LCMB1** complexed Ln(III) to form a luminous complex ("on" state). The binding constant of Eu(III) with closed **LCMB1** was estimated to be 5.0×10^6 by emission titration at 0 °C (Fig. 3a). In contrast, only a weak emission was observed in the presence of a complementary ODN (**fm20**), where the auxiliary units were separated from each other ("off" state) in the extended duplex structure. The emission intensities from both Ln(III) complexes decreased by *ca.* 80% upon addition of **fm20**. Based on the emission intensity, the optimum length of the linker chains tethering the metal chelators to the ODN ends was found to be hexamethylene for the linkers at both the 5′- and 3′-termini. The emission intensity was scarcely affected by modification of the terminus for each of the chelators; the emission intensities were similar for 5′-phen/3′-EDTA-modified and 5′-EDTA/3′-phen-modified LCMBs (ESI†).

Sequence specificity of the **LCMB1** response was assessed using **mm20**, which has one base mismatch; **mm20** decreased the emission intensity of Eu(III)–**LCMB1** by only 10%. The stem–loop structure of Eu(III)–**LCMB1** did not seem to be opened efficiently by **mm20**.

As shown in Fig. 3b, the emission profiles of **LCMB1** (alone and with **fm20**) in response to temperature changes were completely opposite to those of a traditional MB, as expected. The emission of Eu(III)–**LCMB1** decreased with increasing temperature and was finally extinguished at 80 °C. The changes in the emissions from the Eu(III) complex seemed to be synchronized with melting of the stem–loop structure of **LCMB1**; the emission decreased to *ca.* 50% intensity at around the melting temperature (T_m) of **LCMB1** (45.7 °C). The emission profile of Eu(III)–**LCMB1**/**fm20** shows a maximum value at around the T_m. This behavior corresponded to that of a conventional MB, in which the minimum signal appears at around the T_m.[7] These emission characteristics were reversible for temperature changes (data not shown). This means that the components of the Ln(III) complex (EDTA, phen, and Ln(III)), which were split from each other, reconstructed the luminous complex, with formation of the stem–loop structure of **LCMB1**. The EDTA moiety might keep the Ln(III) loosely complexed even after disruption of the closed structure. This is an essential feature of LCMBs for use as versatile molecular devices with off–on-type responses, as will be discussed below.

For the application of an LCMB as a universal molecular device, we used an interface ODN. Part of the interface ODN is the aptamer sequence for a certain molecule (analyte), and the other part is designed to be complementary to the LCMB. The binding of the interface ODN with the LCMB and with the analyte is mutually exclusive as a result of conformational requirements.[8] It is possible to invert the response of the system to the analyte to a turn-on type by making the LCMB and the analyte compete with each other for the interface ODN, *i.e.*, the structure of the LCMB is expected to change from the duplex (open, "off" state) with the interface ODN to the stem–loop (closed, "on" state) through removal of the interface ODN by the analyte. In the presence of a luminous Ln(III), this process would provide a universal sensing platform, using time-resolved fluorescence measurements with off–on mode responses (Fig. 4).

To verify the utility of Ln(III)–LCMB as a sensing platform, **LCMB2** and the interface ODN, **iATP**, were used to compose an aptamer-based ATP sensor.[9] **iATP** consists of the conservative sequence of ATP aptamers[10] and the complementary sequence for **LCMB2**. NTPs (nucleoside 5′-triphosphates: ATP, UTP, GTP, and CTP) were added to solutions of **LCMB2**/**iATP** and Eu(III),

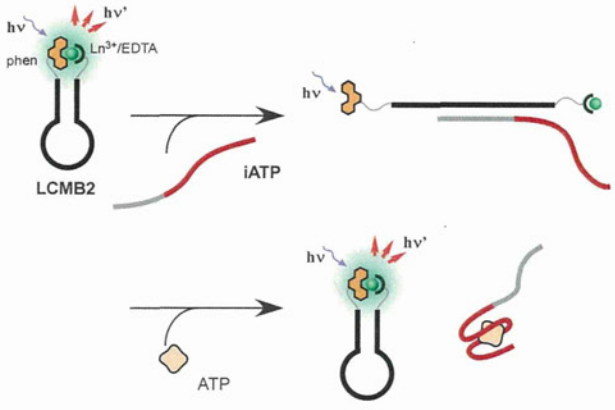

LCMB2 : 5' EDTA–GCGAGAAGTTAGAACCTATGCTCGC–Phen 3'

iATP : 5' ACCTGGGGGAGTATTGCGGAGGAAGGTTCTAACTTC 3'

Fig. 4 ATP sensor consisting of Ln(III)–**LCMB2** and **iATP**. Bold letters in the **LCMN2** and **iATP** sequences are domains that bind to each other. Red letters in the **iATP** sequence are the binding domain to ATP.

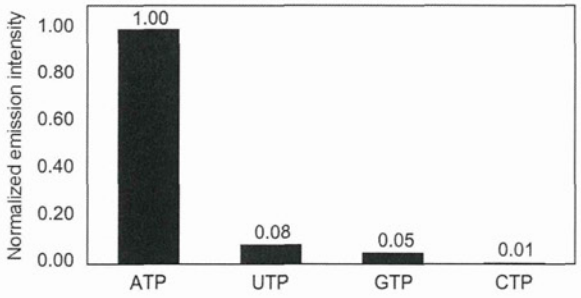

Fig. 5 Normalized emission intensities at 611 nm of solution containing Eu(III)–**LCMB2**/**iATP** in the presence of 20 μM NTPs. Concentrations of **LCMB2**/**iATP** and Eu(III) were 1.0 and 5.0 μM, respectively. The measurements were carried out in a 10 mM HEPES buffer containing 100 mM NaCl and 5 mM $MgCl_2$ (pH 7.0). The excitation wavelength was 280 nm. Delay time and gate time were 50 μs and 2.0 ms, respectively.

and the emission intensities were measured using time-resolved techniques. Upon addition of ATP, the emission intensity of the solution increased to *ca.* six times that before addition. As we expected, ATP seems to remove **iATP** from **LCMB2**, and **LCMB2** restores its closed form, which can form a luminous Ln(III) complex. The normalized emission intensities for the four NTPs are shown in Fig. 5. It is apparent that the emission intensities of the NTPs were essentially unchanged, except in the case of ATP. The observed specificity of **LCMB2** toward ATP could be attributed to the nature of the ATP aptamer in ligand binding, as previously reported by Huizenga and Szostak, suggesting that the intrinsic binding property of the ATP aptamer was preserved even in this system.[10] Although direct modification of fluorescent dye with an aptamer, where the aptamer itself acts as a signalling probe, may carry significant risk of a loss in the original affinity and specificity,[8,11] such a kind of problematic issue could be avoided by the use of interface ODN.

In summary, we demonstrated a universal sensing platform with a time-resolved fluorescence measurement technique. The system was based on allosteric formation of a luminous Ln(III) complex in response to a target molecule. Once their effective aptamers have been obtained, various targets could be covered with this flexible system, using individually designed interface ODNs, even with the same LCMB. Also, the system could be extended to multicolor multiplex assays by preparing specific LCMB–interface ODN combinations for each target, and using them with the associated Ln(III) ions of certain luminescent colors.

This research was partly supported by a Grant-in-Aid for Young Scientists (B) (23750090 to Y.K.) and for Scientific Research on Innovative Areas ("Coordination Programming" Area 2107, No. 24108734 to T.I.) from the Ministry of Education, Culture, Sports, Science and Technology, Japan.

Notes and references

‡ Luminescence lifetime (τ_{Tb} = 1.26 ms and τ_{Eu} = 1.34 ms) and the number of water molecules in the inner coordination sphere (q_{Tb} = 0.17 and q_{Eu} = 0.06) were calculated for similar systems, where the complexes were also formed cooperatively using hybridization of DNA (see details in ref. 1*f*).

1 (*a*) T. Ihara, Y. Takeda and A. Jyo, *J. Am. Chem. Soc.*, 2001, **123**, 1772–1773; (*b*) T. Ihara, T. Fujii, M. Mukae, Y. Kitamura and A. Jyo, *J. Am. Chem. Soc.*, 2004, **126**, 8880–8881; (*c*) Y. Kitamura, T. Ihara, K. Okada, Y. Tsujimura, Y. Shirasaka, M. Tazaki and A. Jyo, *Chem. Commun.*, 2005, 4523–4525; (*d*) Y. Kitamura, T. Ihara, Y. Tsujimura, M. Tazaki and A. Jyo, *Chem. Lett.*, 2005, 1606–1607; (*e*) Y. Kitamura, T. Ihara, Y. Tsujimura, Y. Osawa, M. Tazaki and A. Jyo, *Anal. Biochem.*, 2006, **359**, 259–261; (*f*) Y. Kitamura, T. Ihara, Y. Tsujimura, Y. Osawa, D. Sasahara, M. Yamamoto, K. Okada, M. Tazaki and A. Jyo, *J. Inorg. Biochem.*, 2008, **102**, 1921–1931; (*g*) T. Ihara, Y. Kitamura, Y. Tsujimura and A. Jyo, *Anal. Sci.*, 2011, **27**, 585–590.

2 (*a*) J. Brunner and R. Kraemer, *J. Am. Chem. Soc.*, 2004, **126**, 13626–13627; (*b*) F. H. Zelder, J. Brunner and R. Krämer, *Chem. Commun.*, 2004, 902–903; (*c*) N. Graf, M. Görtiz and R. Krämer, *Angew. Chem., Int. Ed.*, 2006, **45**, 4013–4015.

3 (*a*) D. M. Kolpaschikov, *Chem. Rev.*, 2010, **110**, 4709–4723; (*b*) X.-H. Chen, A. Roloff and O. Seitz, *Angew. Chem., Int. Ed.*, 2012, **51**, 1–6; (*c*) H.-C. Yeh, J. Sharma, J. J. Han, J. S. Martinez and J. H. Werner, *Nano Lett.*, 2010, **10**, 3106–3110.

4 (*a*) S. Pihlasalo, J. Kirjavainen, P. Hänninen and H. Härmä, *Anal. Chem.*, 2011, **83**, 1163–1166; (*b*) A. Tsourkas, M. A. Behlke, Y. Xu and G. Bao, *Anal. Chem.*, 2003, **75**, 3697–3703; (*c*) L. N. Krasnoperov, S. A. E. Marras, M. Kozlov, L. Wirpsza and A. Mustaev, *Bioconjugate Chem.*, 2010, **21**, 319–327.

5 (*a*) N. Sabbatini, M. Guardigli and J.-M. Lehn, *Coord. Chem. Rev.*, 1993, **123**, 201–228; (*b*) J.-C. G. Bünzli and C. Piguet, *Chem. Soc. Rev.*, 2005, **34**, 1048–1077; (*c*) I. Hemmilä and V. Laitala, *J. Fluoresc.*, 2005, **9**, 529–542; (*d*) L. J. Charbonnière, *Curr. Methods Inorg. Chem.*, 2011, **1**, 2–16.

6 (*a*) G. Wang, J. Yuan, K. Matsumoto and Z. Hu, *Anal. Biochem.*, 2001, **299**, 169–172; (*b*) A. Oser and G. Valet, *Angew. Chem., Int. Ed. Engl.*, 1990, **29**, 1167–1169; (*c*) S. Sueda, T. Ihara, B. Juskowiak and M. Takagi, *Anal. Chim. Acta*, 1998, **365**, 27–34; (*d*) J. Coates, P. G. Sammes, G. Yahioglu, R. M. West and A. J. Garman, *J. Chem. Soc., Chem. Commun.*, 1994, 2311–2312.

7 For example: (*a*) G. Bonet, S. Tyagi, A. Libchaber and F. R. Kramer, *Proc. Natl. Acad. Sci. U. S. A.*, 1999, **96**, 6171–6176; (*b*) S. Tyagi and F. R. Kramer, *Nat. Biotechnol.*, 1996, **14**, 303–308; (*c*) S. A.-E. Marras, S. Tyagi and F. R. Kramer, *Clin. Chim. Acta*, 2006, **363**, 48–60.

8 (*a*) N. Li and C.-M. Ho, *J. Am. Chem. Soc.*, 2008, **130**, 2380–2381; (*b*) R. Nutiu and Y. Li, *Angew. Chem., Int. Ed.*, 2005, **44**, 1061–1065; (*c*) B. Juskowiak, *Anal. Bioanal. Chem.*, 2011, **399**, 3157–3176.

9 (*a*) R. Nutiu and Y. Li, *J. Am. Chem. Soc.*, 2003, **125**, 4771–4778; (*b*) M. Zhang, S.-M. Guo, Y.-R. Li, P. Zuo and B.-C. Ye, *Chem. Commun.*, 2012, **48**, 5488–5490; (*c*) J. Zheng, J. Li, Y. Jiang, J. Jin, K. Wang, R. Yang and W. Tan, *Anal. Chem.*, 2011, **83**, 6586–6592; (*d*) Z. Tang, P. Mallikaratchy, R. Yang, Y. Kim, Z. Zhu, H. Wang and W. Tan, *J. Am. Chem. Soc.*, 2008, **130**, 11268–11269.

10 D. E. Huizenga and J. W. Szostak, *Biochemistry*, 1995, **34**, 656–665.

11 (*a*) S. Beyer, W. U. Dittmer and F. C. Simmel, *J. Biomed. Nanotechnol.*, 2005, **1**, 96–101; (*b*) S. Jhaveri, M. Rajendran and A. D. Ellington, *Nat. Biotechnol.*, 2000, **18**, 1293–1297.